Department of Chemistry, University of Jyväskylä

SPECTROSCOPIC STUDIES ON LIGHT-HARVESTING COMPLEXES OF GREEN PLANTS AND PURPLE BACTERIA

JANNE IHALAINEN

Academic Dissertation
for the Degree of
Doctor of Philosophy

Jyväskylä, Finland 2002

Research Report No. 92

DEPARTMENT OF CHEMISTRY, UNIVERSITY OF JYVÄSKYLÄ
RESEARCH REPORT No. 92

SPECTROSCOPIC STUDIES ON LIGHT-HARVESTING COMPLEXES OF GREEN PLANTS AND PURPLE BACTERIA

By

JANNE IHALAINEN

Academic Dissertation
for the degree of
Doctor of Philosophy

To be presented, by permission of the Faculty of Mathematics and Science of the University of Jyväskylä, for public examination in Auditorium KEM 4, on September 7th, 2002, at 12 noon.

Jyväskylä, Finland
ISBN 951-39-1265-5
ISSN 0357-346X

URN:ISBN:978-951-39-9883-7
ISBN 978-951-39-9883-7 (PDF)
ISSN 0357-346X

Jyväskylän yliopisto, 2023

Preface

This thesis describes spectroscopic studies on photosynthetic light-harvesting systems carried out in the years 1998 - 2002 at the Department of Chemistry, University of Jyväskylä.

I am most grateful to my supervisor Prof. Jouko Korppi-Tommola for giving me the freedom to find my own research topic and way of pursuing the degree of Doctor of Philosophy and so to become acquainted with the science of photosynthesis. I wish also to express my gratitude to my co-workers in Jyväskylä for the good times we spent together in the coffee "box", in the woods, and in the city. Especially, I wish to thank Dr. Pekka Lehtovuori, Pasi Myllyperkiö, and Prof. Jussi Eloranta for their patient guidance of my "small" computer problems; Jani Kallioinen, Viivi Lehtovuori, Janne Savolainen, and again Pasi Myllyperkiö for sharing lab times with me; and Juha Linnanto for constructive debates on the light-harvesting processes in photosynthetic systems.

In the course of the work, close ties were established with the physics departments of the Free University Amsterdam and the University of Tartu. The visits to Amsterdam to Prof. Rienk van Grondelle's group were always delightful and educational, and I especially enjoyed (and still do) the frank approach that prevails in Rienk's group. Thank you, Rienk. I want to express warmest thanks to all my colleagues in Amsterdam, and especially to Bas Gobets, who introduced me to the secrets of the streak camera and I introduced him to the secrets of low temperature hiking. Special thanks are also owed to Dr. Jan Dekker and Dr. Ivo van Stokkum who played important roles in a number of the articles of this thesis.

I also enjoyed visits to Tartu and I wish to thank Dr. Arvi Freiberg whose active and enthusiastic approach to science was a joy to experience and Dr. Margus Rätsep with whom I had the pleasure of working.

Without the samples put at my disposal, this thesis would not exists. I am very grateful to all those who supplied samples for the projects of this work: Dr. Roberta Croce and Prof. Roberto Bassi, Dr. Poul-Erik Jensen and Prof. Henrik Vibe Scheller, Dr. Beate Ücker and Prof. Hugo Scheer. Also deserving mention are Dr. Elena Bergo and Prof. Roberto Barbato who instructed me in the isolation processes for light-harvesting antenna.

Ms. Kathleen Ahonen is thanked for careful and instructive revision of the language of this thesis.

A scholarship from the graduate school of the University of Jyväskylä was greatly appreciated. The visits to Free University Amsterdam were mainly supported by the European

Science Foundation via the Biophysics of Photosynthesis and ULTRA programmes and the visits to the University of Tartu were supported by the EC Center of excellence program "EstoMaterials".

Finally, deepest thanks to my dear Tiinamari who has been beside me all these years and supported me whenever necessary. Although times were not always easy, we managed to pull through. One milestone has been reached, and the next and more important ones are waiting.

Espoo, June 2002

Janne Ihalainen

Abstract

Light-harvesting properties of light-harvesting complex 2 (LH2) from purple bacterium *Rhodospirillium (Rs.) molischianum* and antenna complexes of green plant photosystem I (PSI) were characterized by spectroscopic methods.

LH2 is a peripheral antenna protein complex that absorbs light, i.e. collects excitation energy, for chemical reactions of purple bacteria. The collection of sunlight is performed by bacteriochlorophylls organized as two separate rings, named as B800 and B850 according to their absorption maxima. Steady-state absorption properties of isolated LH2 complexes were characterized and the rate of excitation energy transfer between the B800 and B850 rings was determined by transient absorption technique.

Green plant PSI has two antenna complexes, light-harvesting complex I (LHCI) and PSI-core antenna, which are bound together forming a complex called PSI-200. The isolated LHCI proteins appear in dimeric forms and these dimers were characterized by means of (polarized) steady-state absorption and fluorescence spectroscopy at low temperatures. The preparation was shown to contain a mixture of two spectroscopically different dimers evident in two distinct fluorescence emission maxima.

Both LHCI and PSI-core antenna have a number of strongly coupled pigments with lower excitation energy than that of the primary electron donor, P700, of PSI complex. These low energy bands were further characterized, both in separated (LHCI or PSI-core antenna) and in whole (PSI-200) form, in terms of phonon coupling, phonon mean frequencies, and inhomogenous broadening by using site-selective fluorescence and absorption (hole-burning) techniques.

The green plant PSI-core complex consists of at least 14 different protein subunits. The pigment organization of small subunits (PSI-G, PSI-K, PSI-L, and PSI-N) of PSI-core antenna were determined and the influence of the subunits on the energy transfer properties of PSI-200 complex was investigated. Time-resolved fluorescence technique revealed the excitation energy transfer times between various pigment pools and the excitation energy trapping times in the PSI-200 complex.

List of original publications

This thesis is based on the following publications:

I Janne A. Ihalainen, Juha Linnanto, Ivo H.M. van Stokkum, Pasi Myllyperkiö, Beate Ücker, Hugo Scheer, and Jouko E.I. Korppi-Tommola: Energy Transfer in LH2 of *Rhodospirillum molischianum*, studied by subpicosecond spectroscopy and configuration interaction exciton calculations. *J. Phys. Chem B* 2001, 105, 9849-9856.
https://doi.org/10.1021/jp010921b

II Janne A. Ihalainen, Bas Gobets, Kinga Sznee, Michaela Brazzoli, Roberta Croce, Roberto Bassi, Rienk van Grondelle, Jouko E.I. Korppi-Tommola, and Jan P. Dekker: Evidence for Two Spectroscopically Different Dimers of Light-Harvesting Complex I from Green Plants. *Biochemistry* 2000, 39, 8625-8631.
https://doi.org/10.1021/bi0007369

III Janne A. Ihalainen, Margus Rätsep, Poul Erik Jensen, Henrik Vibe Scheller, Roberta Croce, Roberto Bassi, Arvi Freiberg, and Jouko E.I. Korppi-Tommola: Phonon Couplings of Red Chlorophyll States of Green Plant PSI complex: A Site-Selective Spectroscopy Study. Manuscript to be submitted
https://doi.org/10.1021/jp034778t

IV Janne A. Ihalainen, Poul Erik Jensen, Anna Haldrup, Ivo H.M. van Stokkum, Rienk van Grondelle, Henrik Vibe Scheller, and Jan P. Dekker: Pigment Organization and Energy Transfer Dynamics in Isolated Photosystem I Complexes from *Arabidopsis thaliana* depleted of the PSI-G, PSI-K, PSI-L or PSI-N Subunit. *Biophysical Journal.* In Press
https://doi.org/10.1016/S0006-3495(02)73979-9

Abbreviations

(B)Chl (bacterio)chlorophyll

B800-850 antenna complex of purple bacteria, absorption bands at 800 and 850 nm

β-DM n-dodecyl β,D-maltoside

CD circular dichroism

CI configuration interaction calculation method

DAS decay associated spectrum

EET excitation energy transfer

ESA excited state absorption

FLN fluorescence line-narrowing

fwhm full width at half maximum

IDF inhomogeneous distribution function

LD linear dichroism

LHC light-harvesting complex

OD optical density

PS photosystem

PW phonon wing

Rb. rhodobacter

RC reaction center

Rps. rhodopseudomonas

Rs. rhodospirillum

RT room temperature

S Huang-Rhys factor

SADS species associated difference spectrum

SE stimulated emission

ZPL zero-phonon line

Table of Contents

Chapter One

1 Introduction

Life on earth depends on solar energy. In photosynthesis— conversion of solar energy into chemical energy takes place in photosynthetic organisms plants, algae, and some bacteria. Photosynthesis can be divided into two processes: light reactions and carbon fixation reactions (dark reactions). The light reactions are driven by light, while the dark reactions are driven by the products of the light reactions and they also work in darkness. Only the light reactions are discussed in this thesis, and more precisely, only the light-harvesting processes that give rise to the light reactions.

Light harvesting and excitation energy transfer (EET) for chemical reactions are essential processes in photosynthesis. Under certain conditions, these processes work with more than 90% quantum efficiency. The aim of this study was to deepen understanding of the mechanisms of energy transfer in photosynthetic complexes. Steady-state and ultrafast time-resolved spectroscopic techniques are highly suitable for the purpose, in allowing investigation of the energies, nature, and reactions of excited states of molecular systems. A number of steady-state and time-resolved spectroscopic methods were applied to study the excitation energy level configurations and EET properties of the light-harvesting complex 2 (LH2) of purple bacterium *Rhodospirillium (Rs.) molischianum* and the light-harvesting complexes of green plant photosystem I (PSI-200).

LH2 antenna complex from *Rs. molischianum* is a rather simple protein complex and as its crystal structure is known it is a good target for comparing theoretical calculations and experimental results and determining the energy transfer mechanisms of such photosynthetic complexes. In the work with purple bacterium LH2, a good correspondence was found between the steady-state and transient absorption data and calculations with the configuration interaction exciton method.

Green plant photosystems are far more complex than the photosystems of purple bacteria and important factors for understanding the light harvesting and EET properties in green plants still need to be determined. Studies with green plant PSI-200 complexes, the nature

of special low energy states, excitation equilibration rates, and the influence of several small subunits of the complex on the spectroscopic properties of PSI-200 were determined.

The main reactions of photosynthesis and of the studied complexes are introduced below. Chapter two describes, without extensive theoretical explanations, the methods that were employed. The results of the studies are summarized in Chapter three while more precise descriptions of the studies and the results are presented in the attached reprints of the publications.

1.1 Photosynthesis: the main reactions

In oxygenic photosynthesis, which is the most advanced form of photosynthesis, solar energy is trapped and carbohydrates are synthesized from CO_2 and H_2O, while at the same time O_2 is released into the atmosphere. Overall, oxygenic photosynthesis can be described by an oxidation-reduction reaction:

$$nCO_2 + nH_2O \xrightarrow{\text{Light}} nO_2 + (CH_2O)_n$$

Figure 1 shows, schematically, the linear electron/proton chain from H_2O to NADPH and the creation of H^+ gradient which allows ATP synthesis. These processes are the major light reactions which are driven by solar energy. The electrochemical potential generated during the processes is then used for ATP synthesis. The reduced chemically energy-rich molecules, NADPH and ATP, are used to drive carbon dioxide fixation (dark reactions).[1-3] Four major protein complexes, Photosystems I and II (PSI and PSII), cythocrome b_6f, and ATP synthase, which are embedded in the thylakoid membrane, perform these processes in photosynthesis. Overall, more than 60 different polypeptides are responsible for all required functions for photosynthetic light reactions: light-harvesting, electron transfer, proton translocation, and enzymatic catalysis.[4,5]

Plant photosynthesis is believed to have originated about three hundred million years ago, and the much simpler photosynthetic systems that preceded oxygen evolving systems—photosynthetic green filamentous, purple, and green sulfur bacteria and cyanobacteria—are about three billion years old.[6,7] The plant PSII reaction center (RC) strongly resembles that of the purple bacteria, whereas the PSI RC has a close relation to the RC

of green sulfur bacteria and heliobacteria.[8,9] However, all RCs show striking similarities in composition and kinetics of the electron transfer chains. Studies on bacterial systems have been very fruitful, especially in the case of purple bacteria photosynthesis, and considerable understanding of the primary steps of light-driven energy conversion has been gained in the past decades (see e.g. Blankenship et al.).[10]

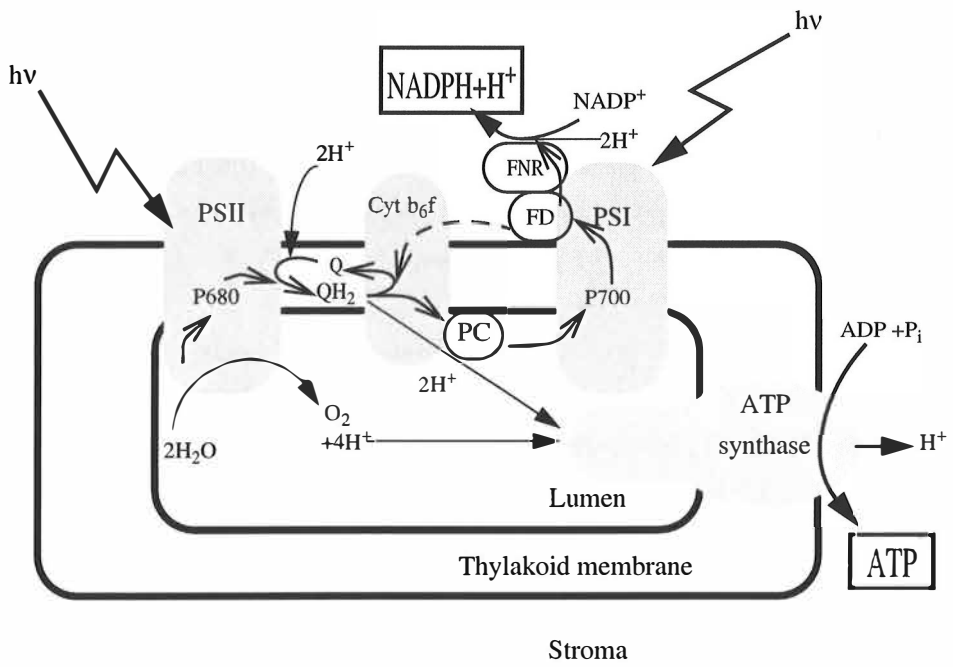

Figure 1. Schematic illustration of electron/proton transfer (thicker/thinner arrows, respectively) in oxygenic photosynthesis. When PSI or PSII absorbs a photon, the excitation energy is rapidly (less than 200 ps) transferred via antenna systems to the RC, to the P700 (PSI) or to the P680 (PSII). A charge separation takes place in the excited special pair and an electron is donated. Excited P680* donates an electron along an electron transfer chain to the plastoquinone (Q) system, which transfers the electrons in protonated form to cytochrome b_6f complex (Cyt b_6f). This complex reduces plastocyanin (PC). Excited P700*, in turn, donates through several carriers an electron to ferredoxin (FD), which either transfer it to ferredoxin-NADP reductase (FNR) for reduction of $NADP^+$, or in the case of cyclic electron transport back to $Cytb_6f$ complex to increase proton transport (dashed line). The oxidized $P700^+$ is reduced by an electron carried by PC, and $P680^+$ is reduced by electrons released from H_2O splitting reaction. Note that PC diffuses along the thylakoid surface and can accomplish a long-distance electron flow between PSs. Utilizing the electrochemical potential gradient, ATP-synthase transfers protons across the thylakoid membrane to catalyze the synthesis of ATP.(After Lehninger et al.[2] with slight modification)

1.2 Pigments in protein environment

The reactions shown in Figure 1 require energy to increase the energy of electrons derived from H_2O to the levels required to reduce $NADP^+$. This energy is captured by absorption of light via antenna protein complexes. The absorption of photons (light-harvesting), excitation energy transfer, and the first charge transfer together with electron donation are carried out by (bacterio)chlorophylls ((B)Chl) and carotenoids in light-harvesting complexes (LHC). (B)Chls are tetrapyrrolic pigments with a central magnesium atom (Figure 2). Carotenoids are basically linear polyene chains of various lengths with different substitutions in the chain. They may have polar head groups. Both pigments are non-covalently bound to photosynthetic polypeptides and they are organized in LHCs in such a way that ultrafast excitation energy transfer to the RC becomes possible.

A variety of (B)Chls exist in photosynthetic species. Spectroscopic and binding properties of individual chromophores depend on the substituents of the molecule. For example, chromophores of oxygenic photosynthesis, Chl *a* and Chl *b,* are distinguished by the 7-methyl substituent in Chl *a* and by the 7-formyl substituent in Chl *b* (this position is shown with R in Figure 2).[12] Double and single bonds, respectively, between C-7 and C-8 of the ring B and an acetyl (in BChl *a*) substitute instead of vinyl (in Chl *a*) at β-position constitute the main differences between Chl *a* and BChl *a* molecules.

The structural differences are reflected in the absorption (and emission) properties of the chromophores. Chl *a* (Chl *b*) in acetone solution shows a spectrum characterized by a relatively strong Q_y-transition at about 663 nm (642 nm) corresponding to the energy difference between the ground and the first excited singlet state, a weak Q_x-transition at about 578 nm corresponding to the energy difference between the ground and the second singlet excited state, and a strong and broad Soret-band at about 430 nm (451 nm), which is the energy difference between the ground and the higher singlet states of the chromophores, (see van Amerongen et al.[13] and Figures 2 and 3). The Q_x-transitions often overlap with vibronic Q_y-transitions. The dipole strength of Chl *a* is estimated to be about 30 debye^2, depending slightly on the environment.[14] The absorptivity of Chl *a* (Chl *b*) is about 80 $mM^{-1}cm^{-1}$ (50 $mM^{-1}cm^{-1}$) at 661 nm (645 nm) and about 100 $mM^{-1}cm^{-1}$ (132 $mM^{-1}cm^{-1}$) at 430 nm (455 nm).[12] The orientation of the Q_y-absorption transition dipole in Chl *a* is shown in Figure 2. BChl *a* absorbs at around 773 nm (Q_y-transition) with dipole strength of about 55 debye^2 in acetone. The Q_x- and Soret-

bands are located at about 583 nm and below 400 nm, respectively (Figure 3).

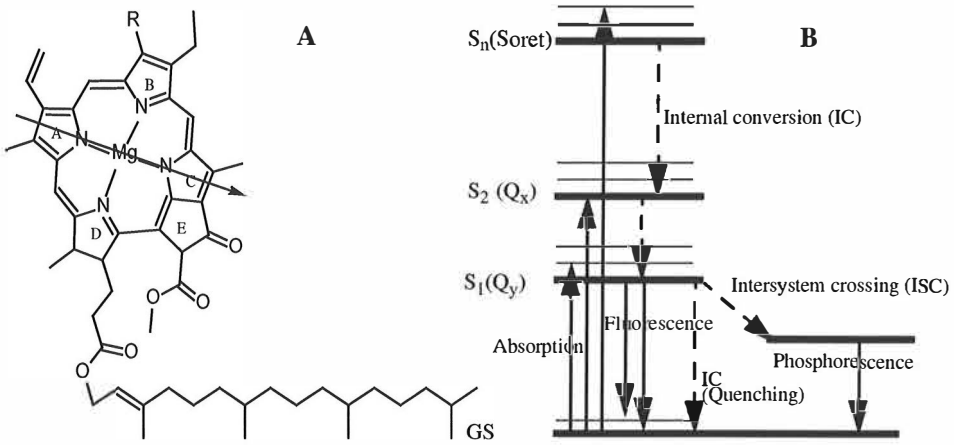

Figure 2. (A) Molecular structure of chlorophyll *a* (where R=CH_3, methyl) and chlorophyll *b* (where R=CHO, formyl). The arrow represents the transition dipole moment of the Q_y-electronic transition, which corresponds to the direction of the transition to the first singlet excited state of the molecule (see e.g. van Zandvoort et al.).[81] (B) Energy level diagram of a chlorophyll molecule showing ground state (GS), singlet excited states (S_1, S_2, S_n), and a triplet state (T). The energies of the singlet states reflect the absorption bands shown in Figure 3. The horizontal thin lines indicate vibronic energy levels and the vertical solid lines radiative transitions.

In most cases the Q_y-absorption band of (B)Chl molecules is red shifted many hundreds of cm^{-1} in protein environment. The spectroscopic shifts may arise from several sources: hydrogen-bonding of (B)Chls with amino acid residues, electro-chromic effects due to charged amino acids in the neighborhood of the chromophore, and often excitonic interactions with neighboring pigments. The excitonic states may be further red shifted as a result of mixing with charge transfer states. Finally, the band width of an electronic transition is very much determined by its coupling to phonons present in the protein environment and to intramolecular vibrations.[13] These effects lead to distinct energy states of particular pigment clusters and in many cases between the pigment clusters excitation energy transfer (EET) is possible. Then excitation energy can be transferred from one protein complex to another, and finally, to the RC for photochemical charge separation.

Good examples of spectral shift effects are the Q_y-absorption bands of BChl *a* in LH2 of purple bacteria (Figure 3 A). Two distinct Q_y-absorption bands are observed in the spectrum,

designated as B800 and B850 according to their absorption maxima. The origin of these bands are the two different pigment rings present in LH2 (see Figure 4).[15] One of these (B800 at about 800 nm, lower ring in Figure 4) has been shown to originate from monomeric pigments and the red shift of about 400 cm^{-1} is caused entirely by the pigment-protein interactions.[15-17] The other band, (B850 at about 850 nm, upper ring in Figure 4), is to a large extent formed from transitions from the ground state to the lowest excitonic E-states of the B850 ring, which are the second lowest excitonic states of the ring (the lowest energy excitonic A-state makes a very weak contribution to the absorption due to symmetry rules of the electronic transitions). The underlying cause of the strong spectroscopic shift in this case is the strong excitonic interaction between the pigments in the ring.[15] In fact, the excitonic states of B850 are not only located at around 850 nm but also at higher and lower, as mentioned above, energies. Although, because of the symmetry rules, these other transitions are of low intensity, but there is no reason why they should not be able to enhance energy transfer between the different pigment clusters in LH2 or energy transfer between LH2 and LH1 (see Paper I and Refs. 16,18).

The excitonic interactions in LHCs from green plants are considered to be rather weak. For example, the red shift of the Q_y-band of Chl molecules in LHCII is very similar in magnitude (300 cm^{-1} - 400 cm^{-1}) to the B800 shift in purple bacteria and is considered to be due to pigment-protein interactions.[19] An exceptionally large spectroscopic shift for the Chl *a* Q_y-transition has been observed for PSI systems from plants, algae, and cyanobacteria. The red-most Q_y-band is located between 700 nm and 720 nm, which is even below the excited state of the RC of PSI (P700). Thus, the shift from absorption maximum of Chl *a* in organic solvent is in the range of 1000 cm^{-1}. The chlorophylls involved in the low energy transition are referred to 'red' pigments. In green plants the pigments with red-most band are located in LHCI, which is a peripheral light-harvesting complex of PSI. An absorption spectrum of LHCI at low temperature is shown in Figure 3 B together with the absorption spectrum of isolated Chl *a*. The physical explanation of the large red shift and of several other unusual spectroscopic features of these pigments is still under debate and is one of the main interests of this thesis too (Papers II and III). Interestingly, Chl *a*-H_2O aggregates have similar absorption and also similar emission properties, than the red pigments in PSI-systems.[20]

Carotenoids, the other main photosynthetic pigments, show a fairly strong absorption in the spectral region between 400 and 600 nm, corresponding to the energy difference between the ground and second singlet excited states.[21] This energy range improves the absorption of visible light in the photosynthetic assembly. The lowest excited singlet state (S_1-state) of

carotenoids lies between 690 nm and 715 nm, but owing to symmetry rules, the transition is forbidden and not distinguishable by classical absorption methods. However, the position of the band has been determined by transient absorption technique.[22]

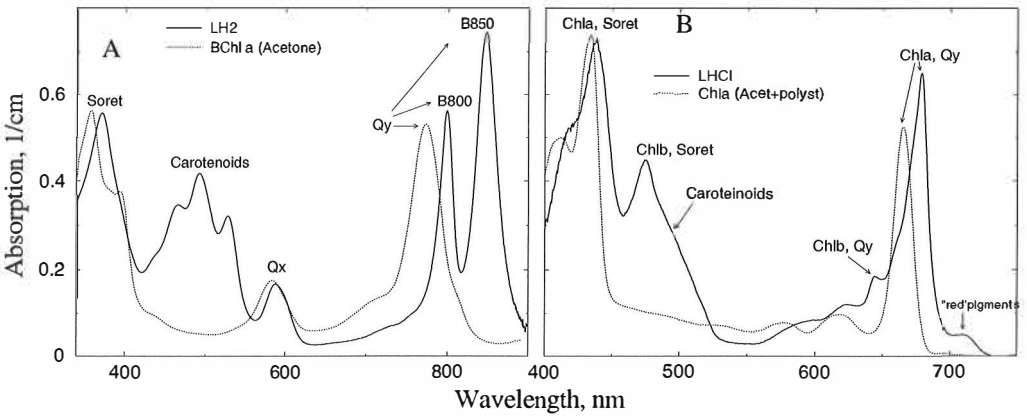

Figure 3. (A) Room temperature absorption spectra of LH2 from *Rhodospirillium Molischianum* (solid) and BChl *a* in acetone (dotted). (B) Low temperature (5 K) absorption of LHCI (solid) from maize and monomeric Chl *a* in polystyrene environment (dashed).

Besides light-harvesting, carotenoids have several other important functions. For example, they play a role as a photoprotector by quenching harmful triplets from (B)Chls. Without their presence in the complexes, ^{3}(B)Chls* would react with oxygen, which would be lethal to the organism.[23] Carotenoids also have a role in non-photochemical quenching, which is a photoprotective function in photosynthetic systems. In green plants and most algal systems, the state of the xanthophyll cycle (zeaxanthin <-> violaxanthin) is an important factor for the dissipation of excess excitation energy.[24,25] Additionally, carotenoids have, just like (B)Chls, a structural stabilizing function in LHCs, and they are needed for proper folding of the light-harvesting polypeptides.[26,27]

1.3 Antenna proteins and light-harvesting

In most cases, photosynthetic complexes contain several different antenna proteins. A large number of these proteins are known. For example, plant systems are known to contain more than ten different antenna proteins. In the 80's and early 90's after successful isolation of individual LHCs, the compositions and nomenclature of the complexes appeared to be

multiplying out of control. One reason was that pigment protein complexes are labile in the presence of detergents, but can not be isolated without them. A reliable qualification of the protein complexes was difficult to carry out, therefore.[28] However, a general consensus has now been reached about the nomenclature and about the pigment composition of the antenna protein complexes and their genes. The names and compositions for plant systems are reviewed in Ref. 29; and the nomenclature for bacterial systems can be found in Refs. 9,12. In this thesis mainly two different kind of the light-harvesting systems were investigated, antenna complexes in PSI from green plants and LH2 from purple bacteria.

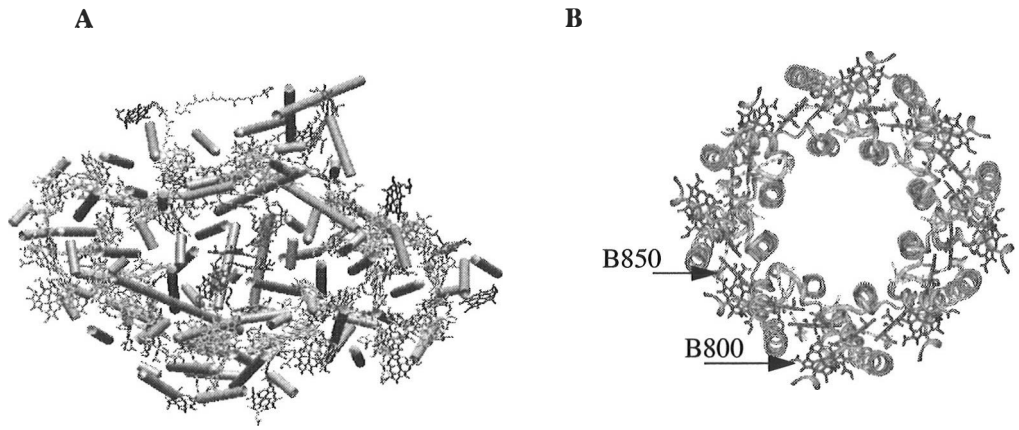

Figure 4. (A) Structural model of PSI from cyanobacterium *Synechococcus elongatus*, view perpendicular to membrane plane. For clarity, only chlorophylls (without phytol tail), carotenoids, and transmembrane α-helixes are shown. The colors of the chlorophylls indicate the coordination to each protein subunit: green PSI-A/B, turquoise -J, blue -K, light blue -L, violet -M, light violet -X, dark red phosphatidylglycerol. The reaction center chlorophylls are marked in red color and the carotenoids in yellow. (B) Structural model of LH2 from purple bacterium *Rhodospirillium Molischianum*, view perpendicular to the membrane plane. Again, only bacteriochlorophylls (without phytol tail), carotenoids (yellow), and α-helixes are shown. The upper ring with 16 bacteriochlorophylls represents the B850 ring (red, tetrapyrrole plane along the view) and the lower, with eight bacteriochlorophylls, forms the B800 ring (blue, tetrapyrrole plane almost towards the view). The structures were obtained from the Brookhaven protein data bank with PDB-codes of 1JB0 for PSI and 1LGH for LH2.[30,31]

1.3.1 Light-harvesting in LH2 of purple bacteria

In purple bacteria the photosynthetic machinery is embedded in the intraplasmic membrane. The construction of this system is far simpler than that of green plant light-harvesting antenna. The major pigments, BChl *a* and BChl *b*, are located in three different

protein complexes: in two light-harvesting antennas and in the RC.[32] The light-harvesting complex I (LH1) surrounds the RC and contains a ring of 32 BChl's, which shows an absorption maximum at about 875 nm (B875 band).[33] In several species, peripheral light-harvesting complexes (LH2) are located next to the LH1 antenna complex.[32] In some purple bacteria in low light or temperature (< 30°C) conditions, part of the LH2 is replaced by LH3 antenna complex, which is thought to increase the efficiency of excitation energy transfer.[34,35] Figure 4 shows that LH2 consists of two BChl *a* rings, in parallel orientation with respect to the membrane. The lower one, designated the B800 ring (shown in blue in Figure 4), has eight or nine BChl *a* molecules. These chromophores absorb maximally at about 800 nm (shown in Figure 3) and they are loosely coupled with each other, as discussed above. The upper ring (shown in red in Figure 4) has 16 or18 BChl *a* molecules. These chromophores are strongly coupled and they are called the B850 (LH2) or B820 (LH3) rings according to their absorption maxima, at 850 nm or 820 nm (Figure 3 B).[15] In addition, the LH2 contain carotenoids which are located between the two BChl *a* rings and are in close contact with the BChl molecules (drawn in yellow in Figure 4.).

A major breakthrough in understanding of the structure-function relations of the complexes was made when the high-resolution crystal structures became available.[31,34,36,37] Additionally, low-resolution structure of LH1 complexes has been obtained by electron-microscopic techniques.[33,38]

The energy transfer properties in purple bacteria are fairly well characterized. At room temperature the EET from the LH2 to LH1 complex takes place in about 3 ps and that from LH1 to RC about 25 - 50 ps, where the charge separation takes place within about 3 ps. A back-transfer from RC to LH1 has been claimed to take place in about 10 ps.[11,39,40]

The most detailed characterization of the EET rates within any photosynthetic unit has been done for LH2. The mechanisms of the energy transfer within the pigment-protein complex and between identical LH2 complexes are still under debate, however. Additionally, no agreement has been reached on the exciton energy level scheme or exciton localization among strongly coupled B850 pigments. A contribution to the discussion of the energy transfer in LH2 complex has been made as part of the present work (Paper I). The energy transfer from B800 to B850, as determined by the transient absorption technique, takes place in the range of 0.7 - 1.0 ps at room temperature and the transfer time increases slightly at lower temperature.[15] If the energy transfer mechanism is considered to be a Förster hopping mechanism[41] and only the obtained absorption bands are taken into account as acceptor states, the calculations produce far

longer EET times than the experimental ones.[42] Recently, in calculations, where the higher optically forbidden states of B850 at around 800 nm are taken into account, more comparable EET times with the experimental ones have been obtained. Thus, the optically forbidden states with higher energy than 850 nm have been suggested enhance the rapidity of the EET (see e.g. Paper I).[43-45]

In purple bacteria excitation energy transfer efficiency from carotenoids to BChls varies from 30% to 90% depending on species.[46-48] The variation has been attributed to the energy difference between the forbidden S_1 state of carotenoids with respect to the Q_y-states of the B800 and B850 rings and to triplet formation efficiency.[46,48] At room temperature the energy transfer from the Car S_1 or S_2 state to BChl Q_y-states (B800 or B850) takes place within about 3-20 ps and 200-300 fs, respectively.[47]

Because of the isoenergy of the states the energy transfer within the BChl rings is rather difficult to determine. In the case of the B850 band, strong coupling between the pigments causes the excitation energy to equilibrate among the B850 pigments very fast, in about 100 fs or less. In the case of the B800 band, overlap of the excited state absorption of the B850 band with the B800 band complicates determination of the B800 intraband energy transfer, and values between 0.5 and 1.0 ps have been suggested.[15]

1.3.2 Light-harvesting in PSI of green plants

PSI is a large protein complex that accepts electrons from plastocyanin and transports electrons through the thylakoid membrane to ferredoxin which reduces $NADP^+$ molecules (Figure 1 and Figure 4). In PSI the reaction center (P700) and internal antenna (called PSI core antenna) are combined in a single Chl-protein complex and the main building block of PSI is a rather large hydrophobic protein complex called PSI-A/B complex. Additionally, PSI has a wide range small subunits (ten in cyanobacteria, 13 in green plants, named as PSI-C to PSI-O) which contribute in many different ways to the function of PSI.[30,49-51] The core complex binds about 100 Chl *a* molecules and about 20 β-carotenoids. Six Chl *a* molecules are considered to be involved in the electron transfer chain and the rest serve as an antenna. A high resolution (2.5 Å) crystal structure of PSI core complex has been resolved only for cyanobacterium *Synechococcus elongatus* (Figure 4 A).[30,51]

In addition to the core complex, green plants and algae have a peripheral antenna complex (LHCI). Green plants have four different kinds of polypeptides, named as Lhca1-

Lhca4, which are located on one side of the core antenna in a dimeric form, with four to five dimers per reaction center.[29,52] Each Lhca polypeptide binds about ten Chls, both Chl *a* and Chl *b* molecules, with Chl *a/b* ratio of about four. Thus, in total LHCI binds about hundred Chls in one PSI-200 unit.

Normally, the spectroscopic properties of PSI, as other photosynthetic complexes, are studied by first isolating it from its membrane environment by detergent treatments and sucrose gradient centrifugation.[53-56] The green plant PSI-200 LHCI can be separated from the core complex by means of the above-mentioned techniques, but owing to similarity of the molecular weights and isoelectric properties, the LHCI dimers have not been successfully separated in native form. For separated dimers, genetic manipulation of the plant systems is required. Recently, reconstituted Lhca1/4 heterodimers have been produced.[57] It is likely therefore that, in the near future, isolated Lhca2 and Lhca3 polypeptides will also be available.

Most of the chlorophylls in PSI have the normal antenna absorption maximum at about 680 nm for Chl *a* and 650 nm for Chl *b* molecules (Figure 3) and the excitation kinetics among these chlorophylls resembles that of the antenna complexes of PSII (see e.g. Ref.13). In spectroscopic terms, PSI pigments with absorption maximum around 680 nm are called 'bulk' pigments. In addition to these, PSI has a certain amount of 'red' pigments, as noted above. The position of the excited red energy level and the number of chlorophylls giving rise to red absorption are variable and depend on the species and growth conditions.[58] Despite their small proportion of the total pigment content in PSI, they overwhelmingly dominate the spectroscopic behavior of PSI complexes. Especially at low temperatures, a large part of the excitation is trapped by the 'red pigments', instead of P700, and red emission between 720 and 760 nm, varying with the species is detected. This effect is illustrated for green plant PSI-200 in Figure 5. As can be seen, below 200 K the excitation energy ends up in the 'red' pigments of either the core complex (F720) or the LHCI (F730) and the fluorescence from these pigment clusters can be detected with lifetimes of 0.6 and 1.9 ns, respectively. Once the temperature rises above 200 K the main part of the excitation is trapped by the RC and the lifetimes of the system are reduced. At room temperature the longest lifetime of PSI-200 is about 120 ps, if the long-lived component that normally originates from uncoupled pigments is disregarded (Paper III).

Polarized transient absorption measurements have shown the single-step energy transfer times between chlorophylls in the PSI antenna to be around 100 - 200 fs, and energy transfer between Chl *a* and Chl *b* molecules in LHCI has two lifetime components, 0.5 and 2-3 ps, similar to lifetimes in PSII antenna proteins.[13,59-62] However, in systems with large amount of (isoenergetic) pigments and their clusters, as in green plant PSI-200, the lifetimes of the

excitation dynamics are determined as 'average' equilibration times. The time needed for excitation to get trapped by the RC for photochemical reaction is then called the trapping time of the system. The equilibration among the 'bulk' chlorophylls in PSI-core complex has been determined to be 500 fs and 5-15 ps between the 'bulk' and 'red' chlorophylls (Figure 6).[58,63] As shown in Figure 5, equilibration time constants are rather insensitive to temperature changes. In contrast, the trapping times change drastically with temperature. At room temperature the trapping time constants have been determined to be about 20 ps for the 'bulk' antenna of core complex, about 20-50 ps for the PSI core complex with part of LHCI (mainly Lhca2/3), and about 120 - 130 ps for the core complex together with the red-most pigments occupying LHCI (mainly Lhca1/4 proteins) (Figure 11 in section 3.3).[64,65] Once the excitation has reached the reaction center the primary charge separation in PSI takes place very fast, with time constants of about 0.8 ps and 9 ps.[66]

Native isolated LHCI samples, and in *E.Coli* reconstituted Lhca1 and Lhca4 polypeptides, have been used to study steady-state spectroscopic and energy transfer properties of LHCI (see e.g. Paper II and Refs. 53,57,61,67). Time-resolved fluorescence experiments have shown that the equilibration between 'bulk' and 'red' chlorophylls in one LHCI monomer takes place in about 4 ps, whereas about 20 ps is needed for equilibration between 'bulk' and 'red' chlorophylls in different monomers in dimeric LHCI.[61,67]

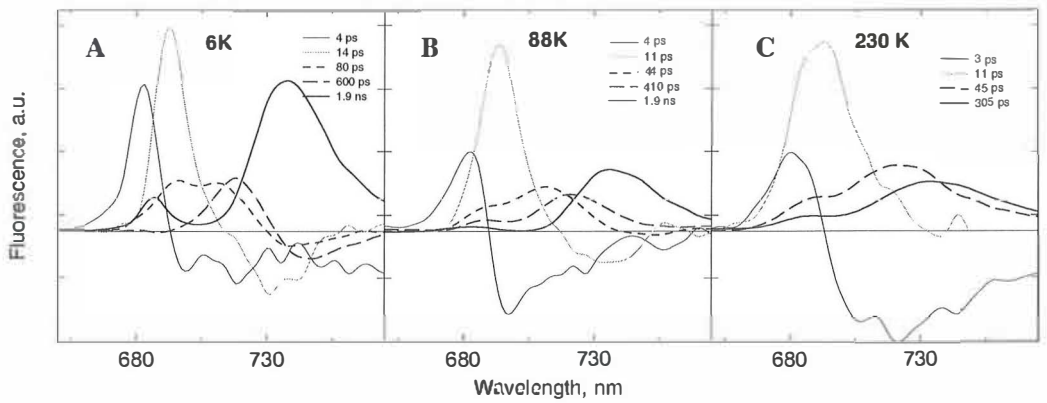

Figure 5. Decay associated spectra of green plant PSI-200 at 400 nm excitation at 5 K (A), 88 K (B), and 230 K (C). The 4 ps component corresponds energy equilibration between 'bulk' and 'red' pigments; the 11-14 ps component also shows energy equilibration but in addition partial trapping by the RC (especially at 230 K); the 50 ps - 300 ps components correspond to trapping by RC. The long lifetimes (about 1 ns or more) at low temperatures originate from F-720 ('red' state of PSI-core complex) or F-730 ('red' state of LHCI).

Despite the many studies, the biological function of the 'red' pigments is still under debate.[11,58,63] One of the first suggestions was that the low-energy states funnel the energy closer to P700 and thereby enhance the excitation trapping of P700.[68] In the recent structural model, the linker dimers B37/38 and A38/39 may be 'red' chlorophylls being near the P700.[30] However, if this is the case, funneling the energy is not the only function, since also the peripheral antenna complex contains 'red' pigments. Another proposal suggests a photoprotective role for the 'red' pigments, which serve as a non-photochemical quencher of excitation in the complex.[69] Recently, Rivadossi et al.[70] have shown that under the 'shadelight' of leaf the 'red' pigments are responsible for 40% of the total photon capture in photosynthetic systems. Thus, a clear enhancement of the absorption cross-section occurs due to long wavelength absorption, which would enhance the energy capture properties of the PSI complex, as suggested by Trissl and Wilhelm.[71] It is worthwhile noting that the presence of 'red' pigments in PSI does not significantly decrease the quantum efficiency of the charge separation, only from 99.6% to 97.6% assuming that the rate of loss to be about $(5\ \text{ns})^{-1}$ and at room temperature trapping takes place within 20 ps without red pigments and within 120 ps with 'red' pigments.

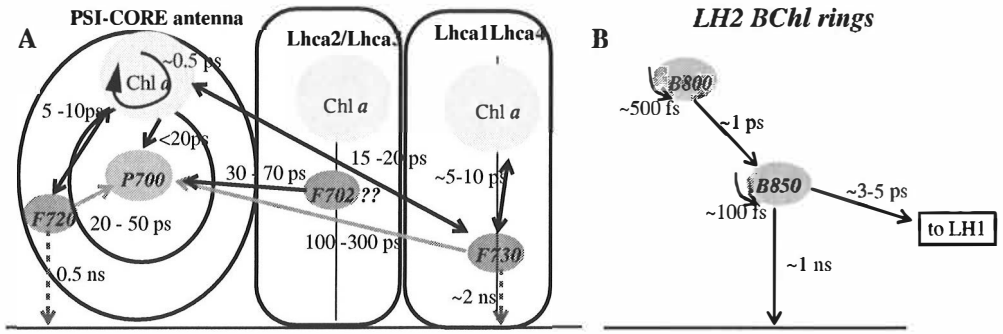

Figure 6, (A) A scheme for excitation energy transfer processes between Chl *a* pigment pools in green plant PSI-200. The dashed lines represent fluorescence lifetimes obtained at low temperature. (B) Excitation energy transfer scheme of purple bacteria LH2. In both schemes the energy scale is arbitrary. The calculated exciton manifold of LH2 of *Rs. molischianum* is shown in Paper I (Figure 3).

Chapter Two

2 Spectroscopic methods

The study of energy transfer and trapping in light-harvesting systems has accelerated markedly in the past ten years, as noted by van Grondelle et al..[11] Several factors explain this: i) more refined isolation methods have been developed for native and active protein complexes from the membrane environment and the vicinity of other photosynthetic proteins, ii) genetic modifications of the photosynthetic systems have been developed, which allow more refined studies of protein complex functions, iii) several isolated protein complexes have been crystallized and structures at atomic resolution have been determined, and iv) the development of Ti:sapphire subpicosecond laser systems offer the possibility to study photosynthetic light-harvesting processes in detail.

In the work summarized here, a number of different spectroscopic methods were applied to characterize isolated photosynthetic complexes. A short description of each method is given below. Emphasis is put on the information obtainable with the method. Detailed theoretical descriptions of the methods and of the light-harvesting processes in photosynthetic complexes can be found elsewhere.[13,35,44,77,78]

Descriptions of the biochemical methods used for isolation and characterization of the studied complexes can be found in Refs. 53,54,75. For the measurements the samples were in buffer solutions with a small amount of detergent added and where necessary, glycerol as cryoprotectant. For the low temperature measurements, a liquid He or N_2 cryostat, designed for spectroscopic measurement was employed.

2.1 Steady-state spectroscopy

Comprehensive knowledge of the steady-state properties of light-harvesting complexes is crucial for understanding their excited-state dynamics and function in their native environment. Thus, a range of steady-state experiments is needed before time-resolved

experiments, the latter then providing information on the lifetimes of the excited states and on dynamics among the states.

Normally steady-state methods are relatively simple and they are easily arranged into the required configuration (see Amesz and Hoff).[79] The light source can be an arc lamp or a laser with suitable emission wavelength range. A monochromator or a spectrograph is used to separate the desired wavelengths, and a charge coupled device (CCD), a photomultiplier, or a light-diode may be used for detection. Polarization optics are easily added to most steady-state spectrometers. Amplifiers (e.g. lock-in amplifiers) can be used for additional sensitivity. Commercial spectrographs are, of course, available, but the experiments of this work were mostly carried out with laboratory-built apparatus.

2.1.1 Absorption, LD, and CD spectroscopy

Measurement of the absorption spectrum is one of the basic methods applied to obtain information about the light-harvesting characteristics of photosynthetic materials. The spectrum contains information on energy and dipole strengths of the excited states of a molecule or a molecular aggregate (coupled system) (Figure 2). The dipole strength is directly related to the well-known experimentally observable molar extinction coefficient ($\varepsilon(\omega)$, $M^{-1}cm^{-1}$).[13]

Because of the presence of different 'pools' of chemically identical pigments or excitonic interactions, the absorption spectra of photosynthetic complexes nearly always consist of strongly overlapping absorption bands, which, moreover are inhomogeneously broadened. When the temperature of the sample is lowered the homogeneous broadening decreases and various spectral bands become more visible. A convenient method to separate the bands is to take a second derivative of the spectrum, which enhances the resolution and facilitates the interpretation of the absorption spectrum.[79]

Additional information on the properties of a system can be obtained by using linearly or circularly polarized light in absorption measurements. In *linear dichroism* (LD) spectroscopy, the signal is determined by the absorption difference between vertically and horizontally polarized light:

$$LD = A_V - A_H \qquad (1)$$

LD spectroscopy can be used to obtain information on transition dipole moments of molecules. In this case, knowledge of the orientation of the molecule with respect to the laboratory axis is needed. Such information has been obtained, for example, for Chl molecules

(Figure 2).[80,81] Conversely, if the orientation of the molecular transition dipole is known with respect to the molecular coordinate system, LD gives information on the orientation of the molecule (in the optimal case) or on the orientation of the transition dipole with respect to the symmetry axes of the sample. This information can be helpful by determining the structure of a protein by means of crystallography or NMR-technique. The LD spectrum is measured from samples where the particles of interest are oriented in a certain laboratory direction. The best orientation of the sample molecules can be achieved naturally by crystallization, but in the case of membrane proteins, the crystallization of those proteins is far from straightforward task. Moreover, in most cases the samples are too dense for spectroscopy. Then, other methods have been applied, like, by stretching a film, using hydrodynamic gradient or strong magnetic or electric field, or applying a gel squeezing technique. The last method was used in this work (Paper II). The sample was placed in a gel (polyacrylamide or gelatin), which was squeezed from opposite directions and allowed to expand perpendicular to the squeezing directions.[79]

A convenient way to present the measured LD signal is as reduced linear dichroism

$$LD_r = \frac{LD}{3A_{ISO}} \qquad (2)$$

where A_{iso} represents the absorption from an isotropic sample (with the same concentration and optical pathlength as the oriented samples). The magnitude of LD_r depends on the angle between the symmetry axes of the particle and the laboratory axes (i.e. orientation of the particle) and on the angle between the transition dipole moment and the symmetry axis of the particle (protein complex).[13] The LD_r is then independent of the absorption intensity, i.e. the dipole strength, and is thus a source of information on the orientation of the transition dipole with respect of the symmetry axis of the protein complex. For disk-like particles (such as LHCII), positive LD_r values indicate the angle between the transition dipole and the symmetry axes of the complex to be larger than the magic angle, whereas negative values mean a smaller angle than the magic angle (54.7^o).[82] In most photosynthetic systems, the symmetry axis of a protein complex is perpendicular to the plane of the complex, i.e. plane of the membrane. Positive LD_r values then indicate the transition dipoles to lie more parallel to the membrane plane (Paper II).[82,83] In most cases, exact values are difficult to obtain because of problems in estimating the orientation factor of the complex. This can be done for complexes with symmetry axes C_n ($n>2$) by means of polarized fluorescence experiments on the oriented complexes.[82,80] Alternatively, the orientation of the transition dipoles and so of the pigments in a protein from

LD signal can be determined with help of low resolution structure of similar kind of protein together with genetic modified samples at the binding sites of the pigments.[84]

It should be noted that only in rare cases do the obtained transition dipole orientations reflect directly the orientation of the pigment in the protein environment even though the knowledge of the orientation of transition dipole of the pigment is known. This is because of the spectral overlap of the differently oriented pigments in the sample, so that the observed LD reflects an 'average' orientation of the pigments absorbing at a certain wavelength.

A *circular dichroism* (CD) spectrum reflects the differential absorbance of the left (A_L) and right (A_R) circularly polarized light of a sample:

$$CD=A_L-A_R \qquad (3)$$

A CD signal can arise from i) asymmetric molecules (chirality), ii) from excitonic interactions between pigments in protein, or iii) from macroscopic aggregated systems where a large number of proteins are bound together.[79] In photosynthetic systems the CD signal from individual pigments (chlorophylls or carotenoids) tends to be very weak and the shape of the spectrum follows the absorption band. The CD signal from excitonic systems is much stronger and arises because the polarization of light changes while interacting with assembled molecules.[13] The peak positions of the excitonic CD bands coincide with the exciton energy levels and the intensity of the signal of each exciton state is proportional to the rotational strength of the state. In the normal case, the excitonic CD spectrum is conservative, meaning that the integral over the CD spectrum is zero. The rotational strength of an excitonic system can be calculated once the coordinates and the transition dipole moments of pigments in the protein are known (see e.g. Pearlstein).[12] Paper I gives the results of calculations of absorption and CD spectra of the LH2 complex from *Rs. molischianum*. A more detailed theoretical description of the calculation method can be found in Ref.16 where the calculations were performed for the LH2 complex from *Rps. acidophila.*

In practice, both LD and CD signals can be detected with the same apparatus, since circularly polarized light can be represented as the sum of two orthogonal linearly polarized beams with a phase shift of $\pi/2$. Hence, it can be constructed from linearly polarized light by positioning a birefringent crystal (transparent material) in 45^o orientation with respect to the plane of the polarization of incident light. By inducing mechanical pressure onto a crystal with a piezoelectronic modulator at suitable alternating voltage, a $\pi/2$ phase shift can be produced, which then results in an alternating left and right circularly polarized light output. If a double voltage is used the phase shift is π and both horizontally and vertically, (plane) polarized light

beams are generated. The polarized light is directed into the sample and the transmitted light, both I and ΔI, is detected. Finally, the signal ($\Delta I/I \propto$ LD or CD) is recorded by using a demodulator, which is synchronized with a piezoelectronic modulator. Both measurements use lock-in-detection as small modulated CD or LD signals are produced on top of the bulk light signal passing through the sample.

2.1.2 Fluorescence spectroscopy

A molecule in an excited state will decay to its ground state via the emission of a photon (fluorescence), internal conversion, intersystem crossing, or a chemical process (quenching) (Figure 2). Thus, emission of photons is a competing process for the primary photochemical events in the conversion of light to chemical energy and fluorescence experiments provide an important tool for photosynthetic research. Such experiments can provide information on the energy of the emitting state relative to the ground state, on lifetimes, or on orientations of transition dipole moments in the excited states. Fluorescence methods can be divided into three groups: i) 'classical' methods, such as measurements of an emission or excitation spectrum and quantum yield, ii) site-selective fluorescence measurements (also called fluorescence line-narrowing spectroscopy), and iii) time-resolved fluorescence measurements. Measurements of polarization effects can be included in every category.[79] All three types of methods were used in this work.

Owing to thermal equilibration the steady-state emission spectrum reflects the excited state configuration of the system. Thus, at low temperatures, EET from short wavelength absorbing pigments to longer wavelength absorbing pigments takes place and the emission bands reflect the longest wavelength (B)Chl states of the system, providing information on the energy and properties of the lowest excited electronic states. The fluorescence excitation spectrum, in turn, displays the relative efficiency of different pigment pools with shorter absorption wavelengths to induce fluorescence. Comparison of the fluorescence excitation spectrum with the absorption spectrum then provides direct evidence of the dependence of the quantum yield on the excitation wavelength, and it therefore reflects on the EET properties of the various pigment pools in the system under study. Care nevertheless must be taken to avoid artifacts, especially in measuring fluorescence quantum yields. This requires estimating of the instrumental light response curves, and self-absorption effects of the sample must be avoided.

In measurements of fluorescence depolarization, orientation of the dipole moments for absorption and emission of the same transition can be taken to be parallel. This means that

polarized fluorescence experiments can be used to study the EET properties of different pigment pools. Anisotropic time-resolved experiments also allow study of the energy transfer dynamics between isoenergetic excited states. In the case of steady-state experiments, rotational diffusion has to be taken into account for protein complexes with molecular weight of 100 kDa or less in aqueous solutions at room temperature,[79] therefore rotational diffusion can be neglected. At low temperatures the molecular rotation effects are not present. Experimentally the anisotropy function can be determined as

$$r(\lambda_{ex}, \lambda_{em}, t) = \frac{I_V(\lambda_{ex}, \lambda_{em}, t) - I_H(\lambda_{ex}, \lambda_{em}, t)}{I_V(\lambda_{ex}, \lambda_{em}, t) + 2I_H(\lambda_{ex}, \lambda_{em}, t)} \quad (4)$$

The monochromator must be corrected with the instrument polarization function for transmission losses for parallel and perpendicular light to obtain correct anisotropy values.[85]

Measurements of anisotropies at several excitations makes it possible to determine the angle ($\alpha_{ex,em}$) between the transition dipole moments of the absorbing and the emitted state with the equation

$$r_{ex,\,em} = \frac{1}{5}(3(\cos\alpha_{ex,\,em})^2 - 1) \quad (5)$$

This shows that the anisotropy values can vary between 0.4 (parallel dipole moments) and -0.2 (perpendicular dipole moments).[13] Further worth noting is that for excitonically coupled dimers the anisotropy value also depends on the coupling strength and in the case of strong coupling $r_{ex,em}$ approaches the value of -0.2 irrespective of the orientation of the dipole moments of the individual pigments. In such a case the two excitonic transition dipole moments are perpendicular when approaching the strong-coupling limit.[13]

2.1.3 Site-selective spectroscopy

Normally, the spectra recorded from pigment-protein complexes are broad and structureless. After non-selective excitation, the spectroscopic bands consist of site-selective (homogeneous) transitions which are distributed along certain energy range (inhomogeneous broadening) (Figure 7A).[13] The inhomogenous broadening arises from many different configurations that proteins may have, so that pigments at particular binding sites of the protein

will have slightly different environments, leading to a distribution of site energies of the pigments. This distribution is assumed to have a Gaussian line shape and a function which mimics the inhomogenous broadening is called an inhomogenous distribution function (IDF).

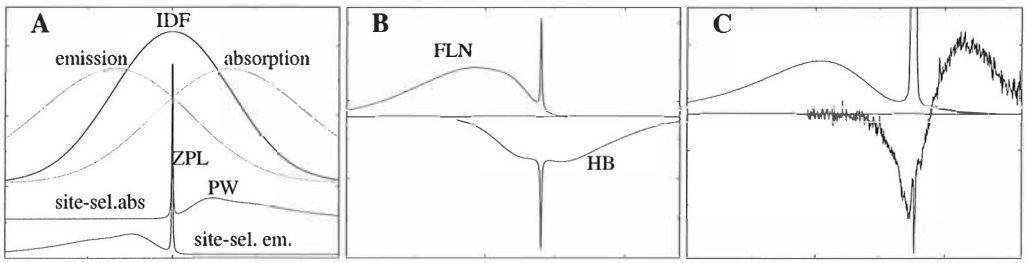

Figure 7. Illustration of results of site-selective spectra. (A) The thick solid line represents inhomogenous distribution function (IDF) and the dotted lines are absorption and emission after non-selective excitation, the thin solid lines represents site-selective absorption and emission spectra after Equation 7. (B) Simulated fluorescence line-narrowing (FLN) and hole-burning (HB) spectra after Equation 8. (C) Measured fluorescence line-narrowing and hole-burning spectra of green plant PSI complex after excitation at about 715 nm. In the case of fluorescence, the scattered laser light is seen instead of ZPL. For the simulations parameters of $S=2.0$; $\nu_m=100$ cm^{-1}; $\Gamma=100$ cm^{-1}; $\gamma=2.0$ cm^{-1}; $\Delta=350$ cm^{-1}; $\nu_B=\nu_c$ were used. See more details below.

The single-site spectrum consists of so-called zero-phonon lines (ZPL) accompanied by phonon wings (PW) (Figure 7A, Equation 7). The PW is a result of coupling of vibrations of the protein environment (phonons) to the electronic transition.[78] The ZPL represents the transition in question without phonon coupling. In general, phonons are responsible for low frequency vibrations, whereas the intramolecular vibrations of pigments appear in the high-frequency spectrum. Each intramolecular vibration results in a new combination of ZPL and PW with a ratio determined by the phonon coupling (see below).

When narrow selective excitation, like continuous laser light with band width of ≤ 1 cm^{-1}, is used for excitation of a molecule in protein environment at low temperature (4.2 K), the inhomogeneous broadening can be circumvented and a site-selective, either absorption (called hole-burning) or emission (called site-selective fluorescence or fluorescence line-narrowing) spectrum, can be measured (Figures 7 B and C). The site-selective emission spectrum mostly describes transitions from the lowest excited state to various vibronic or phonon levels in the ground state and the PW is on the lower energy side of the ZPL. The hole-burning spectra show transitions from lowest energy vibrational state of the ground electronic state to higher vibronic states of excited electronic state. The PW is then located on the high energy side. In addition, a certain number of sites can be excited via their PW, which then results in 'pseudo-PW' on the

lower energy side of the ZPL of the hole-burning spectrum (Figure 7 C). In fact, only the pseudo-PW is obtainable in the hole-burning spectrum because of the anti-hole on the higher energy side of the ZPL. The anti-hole is a result of protein relaxation into another configuration at the excited electronic state (Figure 8).

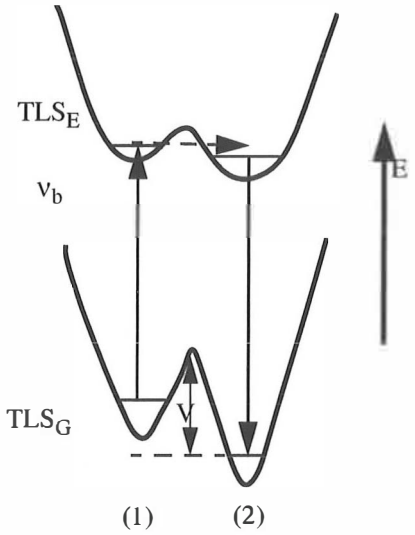

Figure 8. Illustration of non-photochemical hole-burning, using the concept of a two-level system. The two potential wells describe the different environments of a pigment. After excitation at frequency ν_b, the system can relax from the well (1) to the potential well 2, arising a hole in the spectrum at burning frequency ν_b which corresponds the energy difference between ground and excited state of the well (1). Correspondingly, an increase of absorption at energy difference of the well (2) is then also obtained. The latter process is seen as an anti-hole on the higher energy side of the ZPL in the hole-burning spectrum (Figure 7 C).

Normally, in the case of antenna complexes the hole-burning process in the excited state is nonchemical. Hence, it is called a non-photochemical hole-burning technique. The holes are formed primarily by rearrangement of the host environment around the pigment under illumination of laser light (Figure 8).[87] In the measurement of fluorescence, the effect of light on the variation of the ground state configurations as observed in hole-burning is circumvented by using very low excitation flux.

The redistribution of the optical transition between the (phononic) vibronic substates of the electronic excited state and ZPL can be expressed with a so-called Huang-Rhys factor (S), which then describes the strength of the electron-phonon coupling of the system.[86] From a site-selective measurement the S-factor can be determined as follows

$$e^{-S} = \frac{I_{ZPL}}{I_{ZPL} + I_{PW}} \qquad (6)$$

where I_{ZPL} is the integrated intensity of the ZPL and I_{PW} the integrated intensity of the PW. The S-factor of the 0-0 (in the intramolecular vibration bases) transition can not be determined directly from the site-selective emission spectra because of the interference of the ZPL with excitation light. The S-factor can be directly determined in many cases, however, from the hole-burning spectra according to the Equation 6.

In the present work, the measured hole-burning and site-selective fluorescence spectra were simulated by a method introduced by Hayes et al.[89] where a low temperature limit is assumed and no intramolecular vibrations are taken into account. Thus the coupling is restricted to a distribution of protein phonons. The single-site absorption (emission) spectrum can be expressed as

$$L(\nu - \Omega) = \sum_{R=0}^{\infty} \left(\frac{S^R e^{-S}}{R!} \right) l_R(\nu - \Omega \mp R\nu_m) \qquad (7)$$

where S is the Huang-Rhys factor and R is the number of phonons. When R = 0 the transition corresponds to the ZPL, which is assumed to have Lorenzian line-shape. The equation gives the absorption spectrum with the $-R\nu_m$-term and the emission spectrum with the $+R\nu_m$-term.[90] The position and width of the ZPL are expressed with Ω and γ, respectively. Parameter l_R with $R \geq 1$ corresponds to the one-phonon profile with mean frequency of ν_m and width of $R^{1/2}\Gamma$. A Gaussian shape for the one-phonon profile is assumed, since the major contribution to the phonon bandwidth is assumed to be the distribution of the frequencies of the phonon modes. The non-selective absorption (emission) spectrum can be obtained by convoluting the properly normalized single-site absorption (emission) spectrum with the IDF, which was assumed to have a Gaussian line shape with linewidth of Δ. The entire absorption (emission) spectrum after narrow band laser burning (excitation) at ν_B with the illumination time τ can be obtained by using a modified IDF as follows:

$$A_\tau(\nu) = \int d\Omega N(\Omega - \nu_C) e^{-\sigma I \Phi \tau L(\nu_B - \Omega)} L(\nu - \Omega) \qquad (8)$$

where $N(\Omega - \nu_c)$ together with the exponential term corresponds to the modified IDF centered at ν_c. The modified IDF describes the number of sites excited. In this term the single-site has only

$-R\nu_m$ term (Equation 7), independent of whether absorption or emission takes place. The terms σ, I, and Φ are the absorption cross-section, laser intensity, and photochemical quantum yield, respectively. Finally, the hole-burning (or site-selective fluorescence) spectrum is obtained by taking the difference between the A_τ and A_0 terms. Then, by varying several parameters (position and width of IDF, the mean frequency of phonons, and the strength of phonon coupling) the measured site-selective spectra can be simulated and detailed information on the nature of the pigment pools of interest can be collected.

Besides phonon coupling strength and phonon frequencies the non-photochemical hole-burning technique can provide other types of information about pigment-protein systems. IDF functions of various Q_y-states can be determined by measuring ZPL action spectra and EET and electron transfer rates can be determined by measuring width of the ZPL.[88] In the present work the phonon coupling factors of the 'red' states of the PSI complexes were determined (Paper III).

2.2 Time-resolved spectroscopy

Time-resolved spectroscopy is widely used in chemistry, physics, and biology to investigate the dynamics of complex systems. A variety of time scales can be used and the main condition for time-resolved spectroscopic studies is a change in the spectroscopic properties (energy, polarization, or phase) of the studied complex after triggering of a light induced reaction by a short light pulse. In the case of photosynthesis, ultrafast spectroscopy has been used for studies of electron and energy transfer processes in reaction centers and light-harvesting complexes, respectively. These processes often take place on the (sub)picosecond (1 ps = $1*10^{-12}$ s) time scale. It follows that strict requirements are required for the light source to be used in the experiments. A suitable wavelength within the absorption bands of the sample, suitable power, and, most importantly, short enough pulse duration for each studied reaction with reasonable repetition rate of the light source must be available. Today, mainly mode-locked Ti:sapphire laser systems are used, which produce laser pulses shorter than 100 fs with relatively good stability. However, the pulse energies (in nJ-regime) are not in most cases sufficient for spectroscopic measurements and the repetition rate is too high (around 80 MHz) for pump-probe measurements. Amplification of the pulses can be achieved by means of Ti:sapphire amplifiers, pumped with either Q-switched Nd:YAG or Nd:YLF lasers. Pulse energies up to 1.5 mJ, with repetition rate in the kHz-regime, can then be achieved. The output wavelength of the above-mentioned laser system is, however, around 800 nm, which is rather

limited for studies of photosynthetic complexes (Figure 3). The problem can be circumvented by using an optical parametric device (e.g. an optical parametric amplifier, OPA) which, assuming that the device has all the necessary frequency doubling and mixing crystals, is tunable within a wide spectral region, from UV to NIR.[91]

Use of high energy pulses in the study of photosynthetic complexes may cause undesirable effects in the sample. The most common problem is annihilation, which may occur when more than one photon is absorbed by a complex containing a large number of chromophores. In such a case, one excited state (either singlet or triplet) can act as a (mobile) quenching center for other excitations, causing additional decay components in the process under study. These fast components are naturally intensity dependent. Thus, in order to detect decay processes associated with the studied reaction itself, the excitation intensity must be adjusted in such a way that the average number of photons absorbed per complex is less than unity. (Thus, for example, in the case of PSI-200 less than every 200th Chl *a* molecule should be excited!). Moreover, with too high excitation densities, the proportion of radiationless processes may increase, causing local heating of the sample and leading to sample defects. Too high repetition rates should also be avoided because if the studied system has not returned to its initial state (electron back transfer, long-lived excited state relaxations, triplet states etc.) signal accumulation will occur. Rotating or constant flow sample cells are very helpful in avoiding such effects, though they are difficult to use at low temperatures. Moreover, constant flow sample cells are also very protein-sample consuming.

It needs to be noted, too, that if polarization effects are present, such as rotation of a molecule or energy transfer between isoenergetic pigments, magic angle detection must be used either in excitation and detection of fluorescence or in pump and probe measurements. Otherwise decay times obtained from the system are meaningless.

2.2.1 Transient absorption measurements

In transient absorption (or pump-probe) experiments, variation of the absorption with time provides information on the dynamics of the excited states of a sample. In such measurements, subpicosecond time resolution may be easily obtained. In such experiments a short pump pulse first excites the sample and a probe pulse, which is delayed with respect to the pump pulse, is used to monitor differential absorbance of the sample as a function of time. As the speed of light is constant in air, delay of the probe pulse with respect to the pump pulse can be generated by extending the path of the probe light by means of an optical delay line (10 μm

delay corresponds to about 33 fs in time space).

The appropriate wavelength for the excitation depends mainly on the absorption spectrum of the studied system. A suitable wavelength can be obtained by using an OPA or the fundamental frequency or frequency doubled output of the fs-lasers. There are several possibilities for modifying the probe wavelength. In the simplest case, in one-color experiments, the pump and probe pulses are split from the same initial beam and the probe pulse is delayed with respect to the pump pulse. In two-color experiments another OPA is needed to generate the desired wavelength for the probe pulse. However, the whole transient absorption spectrum can be measured when part of the fundamental output of the amplified laser pulse is converted to white light by focusing it into transparent material such as glass, water, or sapphire.[92] The wavelengths can then be separated with a monochromator or optical filters depending on the desired spectral resolution and on the detection system employed, photodiodes or diode arrays. In the case of diode arrays, the group velocity dispersion of white light (different wavelengths propagate with different velocity in transparent media) needs to be taken into account either experimentally or in the final data analysis. If the whole transient spectrum is measured as a function of time, the dynamics of the excited states of the system under study can be determined.

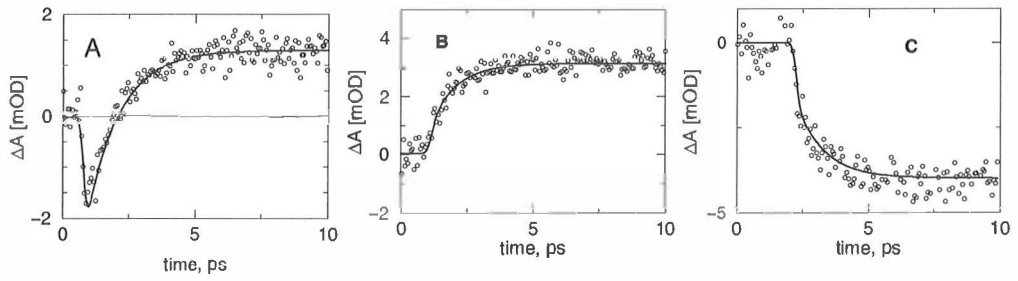

Figure 9. Typical transient absorption traces of LH2 of *Rs. molischianum* after B800 band excitation and detection at 810 nm (A), at 830 nm (B), and at 850 (C). At 810 nm, detection (trace A) consists of ground state bleaching in early moments after excitation and then excited state absorption of the B850 band becomes dominant. At 830 nm (trace B) detection, only excited state absorption is observed. At 850 nm detection the signal consists of both ground state bleaching and stimulated emission of B850 state. (See also Paper I)

There are three origins for the signal in pump-probe measurements: ground state bleaching, stimulated emission (SE), and excited state absorption (ESA). Ground state bleaching is observed when a certain number of molecules are in an excited state (Figure 2 B) during the probing process and the transmission of the sample increases (ΔA decreases). SE

takes place when probe light stimulates the excited state molecules to return to the ground state, which then increases the negative signal. Note that the same probability exists for the stimulated absorption and emission at the emission wavelength. ESA takes place when excited molecules are excited to still higher states by the probe pulse. This naturally decreases the transmission and leads to positive ΔA signal. Thus, all three possible mechanisms must be taken into account in the interpretation of the signal. It is possible that the signals overlap spectrally, complicating the interpretation of the data. In such cases additional information on the sample will normally be required. Reliable models of the excited state reactions can be obtained by combining such information with the time-resolved data.

2.2.2 Time-resolved fluorescence spectroscopy

Time evolution of an emission spectrum an after excitation pulse produces information on the dynamics of the emitting states of a system (section 2.1.2.). Three different techniques can be used for detection of the time-dependent emission properties of a chromophore: *single-photon counting, fluorescence upconversion, and streak camera*. These three techniques, with their advantages and disadvantages, are described below.

The *single-photon counting* (SPC) method is widely used. A time histogram of the emitted photons of the sample is measured by utilizing an old coincidence principle. A reference pulse from a fast photodiode is fed to a constant fraction discriminator that triggers a time-to-amplitude converter (TAC). A stop pulse is fed to the TAC from a fast multichannel photomultiplier tube that sees the first single photon from the sample, and the photons emitted from the sample are then detected as a function of charge in the capacitor or as a function of time.[93] An analog DC signal is created in the TAC and one count is stored in a multichannel analyzer at this voltage. Excitation and data storage are repeated in this way until the histogram of the number of "counts" against each time window is large enough to give a reliable decay curve of emission. The signal to noise ratio is relatively good in this method (dynamic range 1/ 10000) but the time-resolution is low (about 30 ps), mainly due to the electronics of the detector. However, fairly long lifetimes, up to milliseconds, can be measured. By measuring SPC curves at various wavelengths, by using either monochromator or optical filters, global analysis can be applied to analyze the experimental data (see below).

A much better time-resolution than with SPC can be achieved by utilizing the *fluorescence upconversion* technique, which, in principle, is dependent only on the width of the excitation pulse. In this technique the photons emitted from the sample are collected and focused onto a non-linear crystal where a gating beam is also focused. The gating pulse is

delayed with respect of the excitation pulse and the sum frequency of the emitted photons and the gating pulse is detected as a function of the delay between the two pulses. Once the intensity of the gating pulse remains constant the upconverted signal is proportional to the intensity of the fluorescence at each time delay.[79] Various wavelengths of fluorescence can be detected by rotating the crystal, but only a few wavelengths in each measurement set can be detected. In favorable cases the method provides a very high signal to noise ratio (similar to SPC).

A *streak camera* is a very useful device for time-resolved fluorescence measurements and was the main device used in this work. Emission light which contains the entire fluorescence spectrum is collected and focused onto the slit of a spectrograph for wavelength separation. The light is then led to the photocathode of a streak tube where the incident light releases electrons from the photocathode, proportionally to the intensity. The electrons are accelerated in a high voltage field and they fly towards a microchannel plate between a pair of sweep electrodes in perpendicular orientation with respect to the propagation of electrons. A sweep voltage deflects the electrons in different trajectories with respect to their arrival times at the photocathode. The sweep procedure is periodically repeated in phase with the incoming laser pulses. In the multichannel plate, electrons are multiplied several thousand times and they end up at a phosphor screen, where they are reconverted into light and can be detected, for example, with a CCD detector. The main advantage of the streak camera is that when a spectrograph is used the time-dependence of the entire emission spectrum will be obtained at once. The drawback is that its signal to noise ratio is normally less than in SPC or in fluorescence upconversion techniques. The time resolution of the system depends on the sweep rate, which ranges from tens of picoseconds to milliseconds.[92] In measurements of this work the time-resolution was a few picoseconds, which is slightly lower than with fluorescence upconversion measurements but much better than in the SPC systems. In Figure 10 is shown an example of time-resolved emission decay traces together with their fits at two wavelengths, reproduced from a streak camera image.

2.2.3 Data analysis and modeling

In the (sub)picosecond regime, measured time-resolved spectra are always convolutions of the signal from the molecules under study and the instrument response is further a convolution of the exciting pulse and the detector response. Moreover, the time zero is not at the same position for each wavelength because of the group velocity dispersion of light. The shape and duration of the instrument response need to be defined, therefore, either

experimentally or with use of modeling techniques. The instrument response function is needed for deconvolution from the experimental data in order to obtain the kinetics of the system. Experimentally, the instrument response can be determined in pump-probe or fluorescence upconversion experiments by means of cross correlation technique or by utilizing the Kerr effect, in the best case at each experimental wavelength.[92] In fluorescence measurements (streak camera or SPC experiments), scattering of excitation pulses from opaque samples can be used to define an instrumental function. Similarly, by using white light pulses as excitation, the time zero position at each wavelength can be determined. In most cases the measured instrument response is modeled as a Gaussian function and the time zero spectrum as a polynomial function. The spectra of the excitation and detection pulses are needed if exact knowledge is required of the energy levels to be excited and probed (see Paper I and Ref. 45).

Once time-resolved data have been collected for a certain wavelength range a global analysis of the data can be applied. If no knowledge of the kinetic model exists, the first step is to fit the data with a sufficient number of exponential decays and amplitudes for each wavelength and produce decay associated spectra (DAS) (Figure 10). However, although the DAS procedure can be very well used for determining the fluorescence properties and excited state reactions, the spectra and lifetimes obtained do not necessarily represent physical parameters of the system. Rather, the physical parameters of interest are the species-associated absorption/emission spectra (SAAS, SAES or just the species associated spectra SAS), which actually are the real emission or absorption spectra of species present in the sample and the rate constants characteristic of the sample.[79] To obtain information on the physical parameters, a specific model, with spectra of species present and rate constants between the species is fitted to the experimental data. This procedure is also called *target analysis*. In fact, DAS are generally linear combinations of SAES (or SAAS), and only when no excited state reaction occurs do DAS correspond to real physical spectra.

When the system contains a large number of spectral components (as the chlorophylls in antenna complexes do), it is difficult to differentiate between the chromophores. Simplifying assumptions must then be made and, for example, similar spectroscopic behavior of certain chromophore groups can be considered as a single compartment and the kinetics are tested against the experimental data. The level of approximation depends on the quality of the data and availability of additional information on the system. Such an example can be found in Paper I, where the B800 pigments form one grouping of chromophores and the B850 pigments another. It is possible that several different 'partial' models may provide good fits with the data, but they may not represent the true situation in the system. In many cases additional experiments are required to distinguish between various trial models.[79] Moreover, models that fit perfectly well

with the experimental data may contain unrealistic values (e.g. negative fluorescence or rate constants) and such models have to be ruled out. A rule of thumb holds that the simplest model, i.e. least number of subsystems that can reproduce the data should be accepted as the true model describing the system.

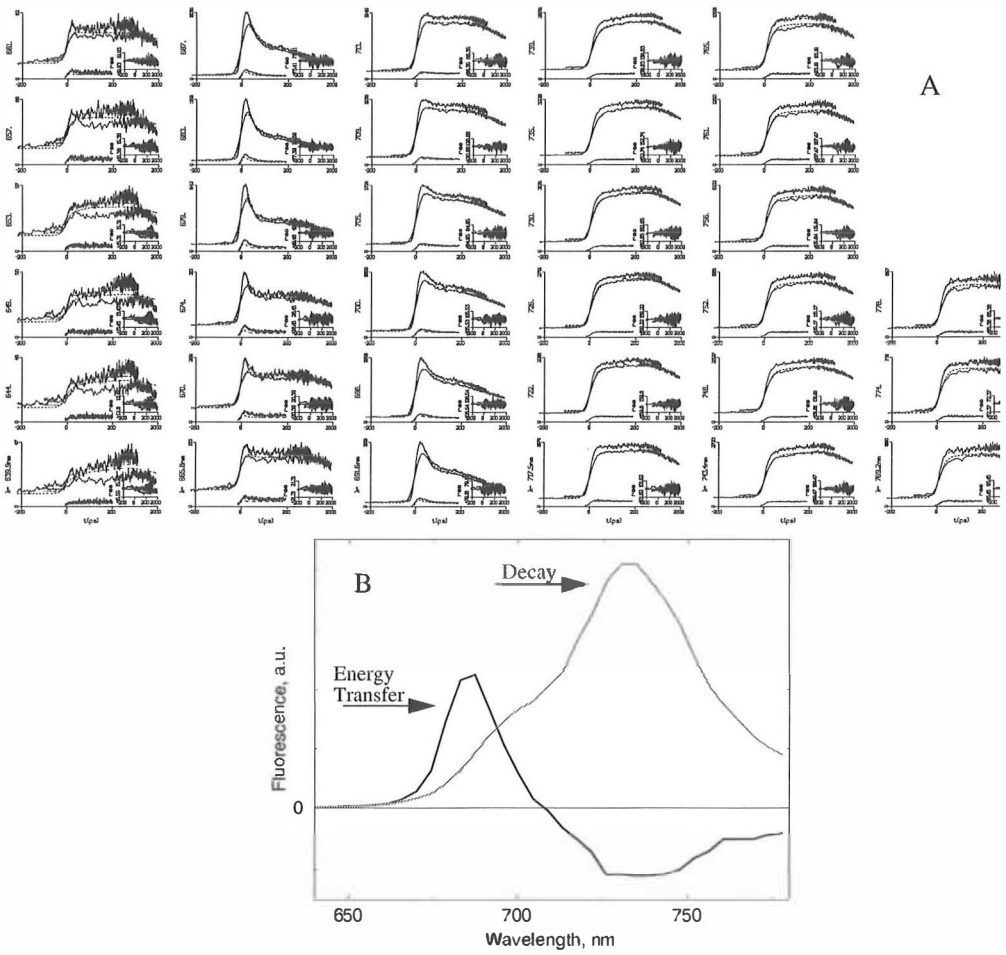

Figure 10. A schematic representation of global analysis for time-resolved fluorescence data. By means of streak camera the detected fluorescence image is split to individual decay traces, with about 4 nm sectors. The three different traces in (A) correspond to the different time ranges that are used. The decay traces are then fitted with a sum of exponentials (dashed lines in (A)). The spectra of amplitudes of each decay time are constructed, which are then called decay associated spectra. In (B) two possible decay associated spectra are shown. Since the positive value corresponds to decay and the negative value to rise of the fluorescence (early times in (A) 678 nm and 730 nm detection, respectively) it is clear that the positive signal on the blue and the negative signal on the red side of the spectrum (B) describe an (excited state) reaction and in this case energy transfer or an energy equilibration process between spectroscopically different pigment pools. A totally positive spectrum means decay of the fluorescence at all wavelengths.

If the collection of data and kinetic analysis are carried out with care, and physical and chemical principles are kept in mind, ultrafast spectroscopy provides a very powerful, in fact the only real tool for studying excited state reactions of complex molecular systems, where these events very often take place on the (sub)picosecond time scale.

Chapter Three

3 Results and Discussion

3.1 LH2 from *Rhodospirillium molischianum*

Owing to its rather simple chromophore organization and the apparent simplicity of its spectral features, LH2 from purple bacteria serves as a good test complex for studies on structure-related EET properties of photosynthetic complexes. Although the structure has been known for a rather long time and a large number of spectroscopic studies have been performed, detailed consensus has not been reached on the excitonic character of the excitation energy levels or on the EET mechanisms of the complex (section 1.3.1 and Paper I). By using the pump-probe technique the EET time from the B800 to B850 ring of LH2 from *Rs. molischianum* was measured to be about 1.0 ps. This is slightly slower than in LH2 complexes from *Rps. acidophila* or *Rs. sphaeroides*. Slight variation of the EET time was observed depending on the excitation wavelength along the B800 band. Clearly faster EET was obtained upon excitation at 830 nm.

On the basis of exciton calculations relying on the atomic structure of the complex, we described in Paper I excitonic states of LH2 from *Rs. molischianum* that explain the steady-state absorption and CD spectra. Moreover, with use of the experimentally measured spectra of the pump and probe pulses, the states that were excited could be specified exactly in the calculations, and by using the same energy level manifold and Fermi's Golden rule, the experimentally determined EET time between the B800 and B850 rings could be explained (Table 1). According to our model, the B850 states $3,4E_3$ at 798 nm and $1,2E_2$ at 824 nm are important routes for the energy transfer from B800 to B850 ring. These findings together with the exciton model could explain the slightly lower EET rate in *Rs. molischianum* than in *Rps. acidophila*. The reason for the different rates in the antenna complexes from the different species is the position of the 'dark' energy levels in the two complexes. In LH2 of *Rs. molischianum*, the $1,2E_2$ states are the only states between the donor B800 and the acceptor B850 states, whereas in *Rps. acidophila* two B850 states ($1,2E_3$ and $1,2E_2$ states) are located in

this region (Paper I and Ref.16).

Table 1: The experimental and calculated lifetimes at several excitation wavelengths corresponding to the excitation energy transfer (EET) from B800 to B850. All transitions from the energy levels excited by the pump pulse were included in the calculations,.

Pump wavelength	Experiment	Calculation
790 nm	1.2 ps	1.3 ps
800 nm	0.9 ps	0.8 ps
810 nm	1.0 ps	0.9 ps
830 nm	0.5 ps	0.4 ps

3.2 Antenna complexes in green plant PSI-200

The green plant photosystems are far more complex than those from purple bacteria. Owing to the complexity and heterogeneity of the complexes, so far only the LHCII from green plants and PSI and PSII of cyanobacterium *Synechococcus elongatus* have been crystallized. Structures have been determined at resolutions of 2.5 Å for PSI, 3.4 Å for LHCII, and 3.8 Å for PSII complex.[26,30,76] Only in the case of the PSI complex was the resolution sufficient for determination of the orientation of the transition dipoles of the chromophores, which is crucial for calculations of the spectrum of the complex. Even isolation of different proteins from the photosystems in native form has turned out to be difficult. Previously, rather harsh detergents like Triton X-100 were used, but nowadays milder detergents like dodecyl maltosides are applied, with better results. In PSI-200, only the core complex can be isolated from the peripheral LHCI (Lhca1-Lhca4) proteins in native form. Further separation of the PSI core complex into individual proteins leads to loss of pigments and thus to denaturation of the proteins. As discussed in section 1.3.2, the LHCI proteins form dimers and, because of their physical similarity, it has not been possible to separate them from each other. In Paper II we noted the spectroscopic divergence between different LHCI dimers. We showed that, in addition to the well-known F-730 band, one of the LHCI dimers emits maximally at 702 nm at 4 K (Figure 11). The assignment of the F-702 band to one of the dimers was made by recording site-selective fluorescence spectra at different excitation wavelengths, where emission intensity varies as a function of the excitation wavelength (Figure 11 B). The intensity of the F-702 band clearly increases relative to the F-730 band upon excitations between 690 and 695 nm, and we concluded that the F-702 and F-730 emissions arise from pigments absorbing at around 690 nm

and 711 nm, respectively. In addition, use of polarized fluorescence techniques showed the red-most band to be a single broad band with no additional spectral substructure.

In previous studies,[94] the LHCI dimers were assigned to LHCI-730 and LHCI-680, according to their low temperature fluorescence maxima. LHCI-730 has been shown to originate at least from the Lhca1/4 heterodimer, but LHCI-680 turned out to be a denatured form produced by monomerization of the other dimers (Lhca2 and/or Lhca3).[57,95]

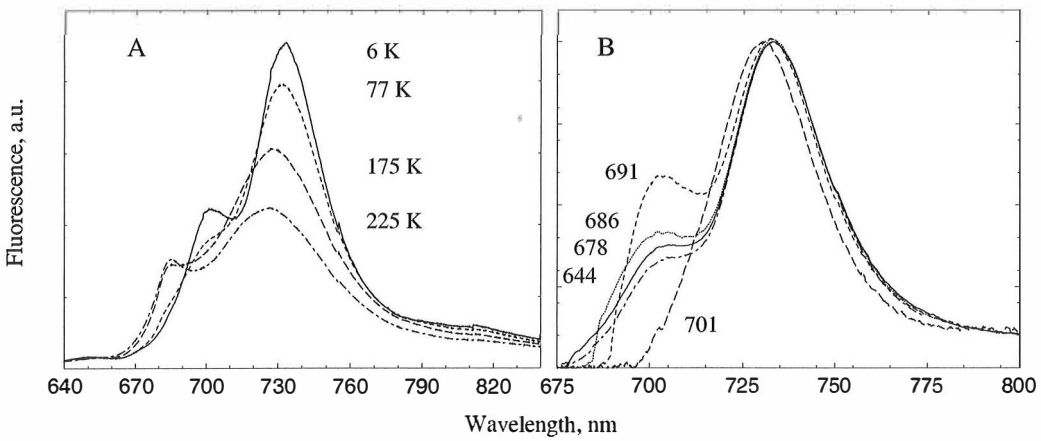

Figure 11. Steady-state emission spectra of isolated LHCI after nonselective excitation at 430 nm at various temperatures from 4 K to 225 K (A). Site-selective emission spectra of LHCI at various excitation wavelengths at 4 K (B). The excitation wavelengths are indicated in the figure and the scattering peaks due to laser light are edited away. See also Paper II.

The finding of spectroscopically different dimers and other steady-state spectroscopic characterization of the dimeric LHCI preparation were used in interpreting the time-resolved fluorescence data obtained by streak camera and fluorescence upconversion techniques.[61] At room temperature the F-702 was assigned to decay within 0.6 ps, whereas the F-730 emission lifetime is about 3 ns. The 0.6 ns component contributes less than 25% amplitude to the total decay, which shows that only the Lhca2 or Lhca3 homodimer has F-702 emission character and that the other homodimer also contributes to the F-730 emission band. Which of the two has the F-702 character probably will be answered once all Lhca-dimers have been biochemically separated. Probably this will be achieved with genetically modified PSI-200 complexes where only selected LHCI dimers are bound to the core complex. Such a system needs to be isolated and purified and the spectroscopic properties characterized. Most likely this will be done in the near future since several successful antisense lines of PSI-200 lacking certain Lhca proteins have already been produced.[96]

The nature of the 'red' pigments is not easy to establish, however. In paper II we concluded that the red most pigments (F-730) are strongly coupled and exhibit exceptionally high inhomogeneous broadening effects. Paper III reported the determination of the strong coupling of the red-most pigments by means of pressure-dependent absorption and emission measurements, which showed about five times as great red shift for the 'red' pigments as for the 'bulk' pigments absorbing around 680 nm, which are weakly coupled. The large pressure induced red shift was then attributed to strong interaction between the 'red' pigments and probably to the charge transfer character of the excited state of those pigments.

As discussed in section 1.3.2, green plant PSI-200 complex contains two different 'red' states, which show low temperature emission maxima at around 720 nm (F-720) and around 730 nm (F-730). F-720 is located in the PSI-core complex and F-730 in LHCI (Figure 6). Note that the F-702 emission band found for the isolated LHCI is strongly quenched in the native PSI-200 complex. An analysis of the phonon coupling of the F-720 and F-730 states was performed by combining the two site-selective spectroscopic measurements, hole-burning and fluorescence line-narrowing, and applying a detailed analysis of the results to the red excited pigments (section 2.1.3). Physical parameters, such as the Huang-Rhys factor (S-factor), mean phonon frequencies, and the broadening and position of IDF of the 'red' pigments of PSI-200 antenna complexes were obtained (Paper III). We showed that the red-most site-selective emission arises from the 'red' pigments of LHCI, in line with the emission maximum of those complexes. However, the hole-burning spectra which are obtained at the red-most absorption band of PSI-200 originate from the 'red' pigments of the PSI-core complex. This is because, at low temperatures, the red-most absorption bands recorded from PSI-core complex and LHCI almost overlap and the 'red' pigments of the core complex have lower electron-phonon coupling (the S-factor is about 2.0 in the PSI-core complex and about 2.8 in the LHCI states; Table 2). An unexpected result was that the absorption and emission bands of the 'red' pigments could not be simulated with the same set of parameters, and one low phonon mean frequency for the hole-burning spectra was required (Table 2). This implies that the potential energy surfaces of the ground and excited states are different. Whether this is due to strong deformation of the lattice or displacement of the pigments, or to some other effect, needs to be clarified. The site-selective absorption and emission spectra for peripheral antennae from PSII (LHCII) could be simulated with the same set of parameters. [90]

Table 2: Simulation parameters for site-selective experiments (FLN for fluorescence line-narrowing and HB for hole-burning experiments) of the PSI-200 complex and its isolated antennas. S corresponds to the Huang-Rhys factor, γ corresponds to the width of the ZPL, ν_m and Γ are the mean frequency and width of phonons, respectively. ν_c and Δ correspond to the position and width of the IDF, respectively. The bottom rows show non-selective absorption and emission maxima simulated with the parameters (Equation 8 and τ=0). The results of the simulations are shown in Figures 4 and 5 in Paper III.

Parameters	PSI-200 FLN	PSI-200 HB	LHCI FLN	PSI-core FLN	PSI-core HB
S	2.6	2.0	2.8	2.0	2.0
γ (cm^{-1})	1.45	1.5	1.45	1.45	1.5
ν_m (cm^{-1})	94	25, 83	93	83	25, 85
Γ (cm^{-1})	142	12, 115	125	115	12, 115
ν_c (cm^{-1})	13790	13970	13825	14045	14045
(nm)	725.2	715.8	723.3	712.0	712.0
Δ (cm^{-1})	340	310	310	310	310
Em_{max} (cm^{-1})	13612	13887	13628	13893	13958
(nm)	734.7	720.1	733.8	719.8	716.4
Abs_{max} (cm^{-1})	13972	14052	14027.5	14123	14123
(nm)	715.7	711.6	712.9	707.8	708.0

3.3 Small subunits in green plant PSI-200

As mentioned in section 1.3.2, the PSI core complex consists of more than ten small (less than 20 kDa) subunits, all of which have specific functions in PSI. In all cases, the functions of the small intrinsic membrane subunits are not known in detail, in particular those that do not occur in the well-characterized PSI complexes from cyanobacteria. One reason for this is that isolation and purification of the subunits from the PSI-core complex in their native form is cumbersome because of the strong interaction between the subunits. The problem can be circumvented by utilizing genetically manipulated plants in which the expression of some subunits has been suppressed.[50] Properties of PSI-200 complexes harvested from mutated plants, lacking a particular PSI subunit, can then be compared with wild-type PSI-200 complex.

In most cases, deletion of a certain subunit does not affect the growth of the plant very much.

Paper IV reports studies of the EET properties of wild-type PSI-200 complex from *Arabidopsis thaliana* carried out by streak camera time-resolved fluorescence techniques. The time-resolved spectra were analyzed globally and the resulting DAS after 475 nm excitation for wild-type PSI-200 complex are shown in Figure 12. The results obtained from the wild-type PSI-complexes were compared with those obtained from PSI-200 complexes devoid of PSI-G, -K, -L, or -N and the influence of those small subunits on the EET was investigated. The pigment composition of the complexes was also studied by low temperature absorption measurements, and well as by high-pressure liquid chromatography (HPLC).

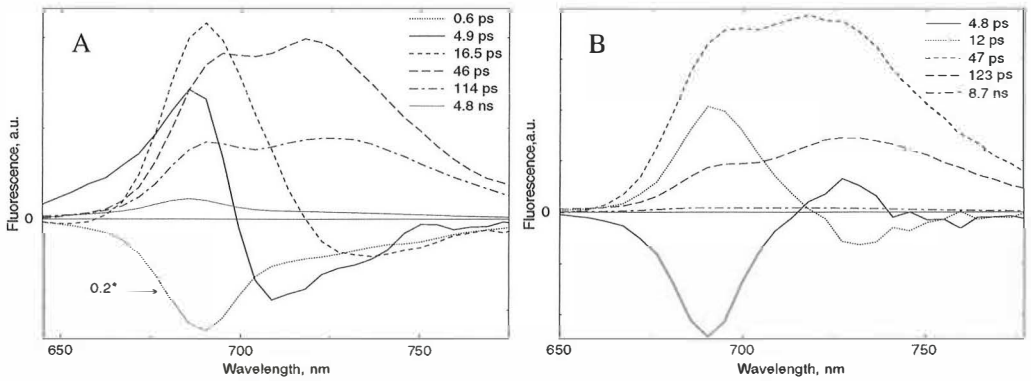

Figure 12. Decay associated spectra (DAS) of fluorescence decay of isolated PSI-200 complexes from wild-type *Arabidopsis thaliana* at room temperature after 475 nm (A) and 710 nm (B) excitation. In both cases about 65% of the excitation energy was absorbed by LHCI and about 35% by the PSI core complex. The 475 nm excited data could be fitted satisfactorily with six components: 0.6 ps (corresponds to Soret-Q_y-transition and Car > Chl *a* EET), 5 ps (excitation equilibrium between 'bulk' and 'red' chlorophylls), 15 ps (equilibrium and possible trapping photons from 'bulk' antenna by RC), 50 ps (trapping, dominated by Lhca2 and Lhca3 complexes, 120 ps (trapping, dominated by Lhca1 and Lhca4 proteins) and >5 ns (long lifetime). Most of the lifetimes were similar in the 710 nm excited data, but the fastest component is, of course, missing and instead of that a 'red'-'bulk' equilibration within about 5 ps is observed. See also Paper IV.

Previously, it has been shown that PSI-L is in close contact with the PSI-H subunit in PSI-200. Thus, PSI-H is also absent when PSI-L is missing from the PSI-200 complex. Recently, PSI-H has been shown to be mainly responsible for the state-transition (various states of LHCII interaction with PSI-200 complex).[97] We showed in Paper IV that PSI-L, together with PSI-H, binds about five Chl *a* molecules absorbing around 667 nm and 688 nm and one or more β-carotene molecules with absorption maximum at 499 nm. It is thus likely that the

chlorophylls that are bound to PSI-L and PSI-H subunits are involved in EET in state 2 when LHCII is possibly docked to PSI core complex. In our experiments, where LHCII are washed out during the sample preparation, the lack of PSI-L and PSI-H subunits did not particularly influence the energy transfer properties of the PSI-200 complex. The only difference in the time-resolved measurements was a lower intensity in the long-living spectrum, which was assigned to originate from the noncoupled pigments of the PSI-200 complex. This can be explained by the rather remote location of the PSI-L and PSI-H pigments relative to the other pigments in the core complex.

The PSI-K and PSI-G subunits have been shown to interact with LHCI proteins.[54,98] In the absence of PSI-K subunit, a partial absence of Lhca2 and Lhca3 proteins from PSI-200 complex was observed by immunoblotting technique,[54] as well as in low temperature absorption spectra, which showed decreased absorption of the Soret Chl *b* band. However, the decreased Chl *b* Soret-absorption blurred possible observations on the carotenoid binding of the PSI-K subunit. The absence of the PSI-G subunit, in turn, does not lead to reduction of the Soret-band absorption and it was shown that PSI-G binds to one or two β-carotene molecules absorbing at 506 and 469 nm. Although the most of the EET properties of the mutants were very similar with those of WT, the absence of either PSI-K or PSI-G subunits leads to small deviations of the EET properties from those of the wild-type PSI-200 complex. As discussed in section 1.3.2 and shown Figures 6 and 12, excitation energy equilibration occurs between the 'bulk' and 'red' pigments within 20 ps, but also trapping by RC takes place in the same time frame (see Figures 6 and 12). The 20 ps trapping contribution is clearly stronger in the PSI-K and PSI-G mutants than in the wild-type PSI-200 complex. This decay process occurs at the expense of the amplitudes of the slower components (50 and 120 ps), which are smaller in the mutants than the wild type. More detailed description of these observations can be found from Paper IV. Since the slower trapping components originate from pigments in both core complex and LHCI proteins (50 ps core complex together with Lhca2 and/or Lhca3 proteins and 120 ps core complex together with Lhca1/4 dimers), it is clear that those subunits are involved in binding of the core complex and the LHCI proteins.

Chapter Four

4 Summary

Steady-state and time-resolved spectroscopic methods were applied to characterize the excitation electronic energies and dynamics of antenna complexes of several photosynthetic systems. The complexes were LH2 complex from purple bacteria *Rs. molischianum* and PSI-core complex and LHCI of PSI-200 from green plants (maize and *Arabidopsis thaliana*). All experiments were performed for biochemically isolated and purified complexes. The experiments were carried out at low temperatures (below 100 K) and at room temperature.

Since most photosynthetic systems function at room temperature, comparison of experimental data with calculated results should be made for room temperature conditions. Such comparisons were made by calculating excitonic levels for purple bacteria LH2 complex and comparing the obtained (in)homogeneously broadened spectra with experimentally measured steady-state absorption and CD spectra. Transition probabilities between various energy levels were calculated using Fermi's Golden rule and assuming the same excitonic level structure that produced the spectra. The EET rates between various spectroscopic states of the system were evaluated and the EET rates between B800 and B850 rings of the LH2 complex were compared with those determined by transient absorption technique. In all cases, agreement between the experimental and calculated values was exceedingly good.

At low temperatures, the homogeneous broadening decreases and the various characteristic spectral bands of different pigment pools are more easily distinguished. The Q_y-absorption levels of LHCI were determined in this way and by using several fluorescence techniques the absorption bands of the two red most emission bands (F-702 and F-730) of LHCI were determined. The F-702 band has not been seen before from the green plant PSI systems. With polarized absorption measurements, the direction of the transition dipole moment of the red-most band was shown to lay almost along the membrane plane, where the proteins are embedded *in vivo*.

In addition, at very low temperatures (around 4 K), by means of site-selective measurements (hole-burning, fluorescence line-narrowing) spectroscopic properties such as the

phonon coupling and mean phonon frequencies and the properties of IDF of pigment-protein complexes can be determined. For the red-most states of green plant PSI-200 complex the phonon coupling was shown to be exceptionally high in the F-730 band of the LHCI and in the F-720 band of the PSI-core complex.

It was shown that by combining advanced molecular biological techniques and spectroscopic tools, detailed information can be obtained on the function of specific subunits in large protein complexes. Use of low temperature absorption measurements together with HPLC analysis allowed determination of pigment contents of PSI-G, PSI-K, PSI-L and PSI-N subunits. The influence of the subunits on the excitation dynamics was then clarified in time-resolved fluorescence experiments with use of the streak camera technique.

REFERENCES

1. Stryer, L. (1988) *Biochemistry* 3rd edition Chapter 22 , W.H. Freeman and Company, New York.

2. Lehninger, A. L., Nelson, D.L., Cox, M.M. (1993) *Principles of Biochemistry* Chapter 18, Worth Publisher, New York.

3. Bower, J.R., Leegood, R.C. (1997) *Photosynthesis* in *Plant Biochemistry* Chapter 2, Dey, P.M., Harborne, J.B. (eds), Academic Press, San Diego.

4. Andersson, B., Barber, J. (1994) Composition, organization, and dynamics of thylakoid membranes, *Advances in Molecular and Cell Biology 10*, 1-53.

5. van Roon, H., van Breemen, J.F.L., de Weerd, F.L., Dekker, J.P., Boekema, E. (2001) Tetrapyrrole photoreceptors in photosynthetic organisms, *Photosynth. Res. 64*, 155-166.

6. Xiong, J. Fischer, W.M., Inoue, K., Nakahara, M., Bauer, C.E. (2000) Molecular evidence for the early evolution of photosynthesis, *Science 289*, 1724-1730. (and a related web page: http://edmall.gsfc.nasa.gov/aacps/news/Photosynthesis.html (Des Marais))

7. Baymann, F., Brugna, M., Muhlenhoff, U., Nitschke, W. (2001) Daddy, where did (PS)I come from? *Biochim. Biophys. Acta 1507*, 291-310.

8. Michel, H., Deisenhofer, J. (1988) Relevance of the photosynthetic reaction center from purple bacteria to the structure of photosystem II, *Biochemistry 27*, 1-7.

9. Neerken, S., Amesz, J. (2001) The antenna reaction center complex of heliobacteria: composition, energy conversion and electron transfer, *Biochim. Biophys. Acta 1507*, 278-290.

10. Blankenship, R.E., Madigan, M.T., Bauer, C.E. (1995) *Anoxygenic Photosynthetic Bacteria*, Kluwer Academic Publisher, Dordrecht.

11. van Grondelle, R., Dekker, J.P. Gillbro, T., Sundström, V. (1994) Energy transfer and trapping in photosynthesis, *Biochim. Biophys. Acta 1187*, 1-65.

12. Scheer, H. (ed) (1991) Chapter 1 (Structure and occurrence of chlorophylls, H. Scheer), Chapter 3 (Bacteriochlorophyll-binding proteins, A.M. Hawthornthwaite, R.J. Cogdell), Chapter 4 (Theoretical interpretation of antenna spectra, R.M. Pearlstein) in *Chlorophylls*. CRC Press, Boca Raton.

13. van Amerongen, H., Valkunas, L., van Grondelle, R. (2000) *Photosynthetic Excitons*, World Scientific Publishing Co. Pte. Ltd., Singapore.

14. Knox, R.S. (2001) Dipole strengths of chlorophyll *a* and bacteriochlorophyll *a*, in *Proceedings of PS2001* Brisbane, S2-008. CSIRO Publishing, Melbourne, Australia.

15. Sundström, V., Pullerits, T., van Grondelle, R. (1999) Photosynthetic light-harvesting: Reconciling dynamics and structure of purple bacterial LH2 reveals function of photosynthetic unit, *J. Phys. Chem. 103*, 2327-2346.

16. Linnanto, J., Korppi-Tommola, J.E.I., Helenius, V.M. (1999) Electronic states, absorption spectrum and circular dichroism spectrum of the photosynthetic bacterial LH2 antenna of *Rhodopseudomonas acidophila* as predicted by exciton theory and semiempirical calculations, *J. Phys. Chem. B 103*, 8739-8750.

17. van Oijen, A.M., Ketelaars, M., Köhler, J., Aartsma, T.J., Schmidt, J. (1999) Unraveling the electronic structure of individual photosynthetic pigment-protein complexes, *Science* 285, 400-402.

18. Koolhaas, M.H.C., Frese, R.N., Fowler, G.J.S., Bibby, T.S., Georgakopoulou, S., van der Zwan, G., Hunter, C.N., van Grondelle, R. (1998) Identification of the upper exciton component of the B850 bacteriochlorophylls of the LH2 antenna complex, using a B800-Free mutant of *Rhodobacter Sphaeroides*, *Biochemistry 37*, 4693-4698.

19. van Amerongen, H., van Grondelle, R. (2001) Understanding the energy transfer function of LHCII, the major light-harvesting complex of green plants, *J. Phys. Chem. B 105*, 604-617.

20. Helenius, V.M., Hynninen, P.H., Korppi-Tommola, J.E.I. (1993) Cholorphyll *a* aggregates in hydrocarbon solution: a picosecond spectroscopy and molecular modelling study, *Photochem. Photobiol. 58*, 867-873.

21. Lichtenthaler, H. (1987) Chlorophylls and carotenoids: Pigments of photosynthetic biomembranes. *Methods Enzymol. 148*, 350-382.

22. Polívka, T., Herek, J.L., Zigmantas, D., Åkerlund, H.E., Sundström, V. (1999) Direct observation of the (forbidden) S_1 state in carotenoids, *Proc. Natl. Acad. Sci U.S.A. 96*, 4914-4917.

23. Cogdell, R.J. (1985) Carotenoids in photosynthesis, *Pure & Appl. Chem. 57*, 723-728.

24. Young, A.J. (1991) The photoprotective role of carotenoids in higher plants. *Physiol. Plant. 83*, 702-708.

25. Horton, P., Ruban, A.V., & Walters, R.G. (1996) Regulation of light-harvesting in green plants, *Annu. Rev. Plan Physiol. Plant Mol. Biol. 47*, 655-684.

26. Kühlbrandt, W., Wang, D. N., Fujiyoshi, Y. (1994) Atomic model of plant light-harvesting complex by electron crystallography. *Nature 367*, 614-621.

27. Plumley, F.G., Schmidt, G.W. (1987) Reconstitution of chlorophyll *a/b* light-harvesting complexes: Xantophyll-dependent assembly and energy transfer, *Proc. Natl. Acad. Sci U.S.A. 84*, 146-150.

28. Green, B. R., Durnford, D.G. (1996) The chlorophyll-carotenoid proteins of oxygenic photosynthesis, *Annu. Rev. Plant Physiol. Plant Mol. Biol. 47*, 685-714.

29. Jansson, S. (1994) The light-harvesting chlorophyll *a/b*-binding proteins, *Biochim. Biophys. Acta 1184,* 1-19.

30. Jordan, P., Fromme, P., Witt, H.T., Klukas, O., Saenger, W., Krauss, N. (2001) Three-dimensional structure of cyanobacterial photosystem I at 2.5 angstrom resolution, *Nature 411*, 909-917.

31. Koepke, J., Hu, X., Muenke, C., Schulten, K., Michel, H. (1996) The crystal structure of the light-harvesting complex II (B800-850) from *Rhodospirillum molischianum*, *Structure 4*, 581-597.

32. Zuber, H., Cogdell, R.J. (1995) Structure and organization of purple bacteria complexes, Chapter XX in *Anoxygenic Photosynthetic Bacteria* Blankenship, R.E., Madigan, M.T., Bauer, C.E. (eds), Kluwer Academic Publisher, Dordrecht

33. Karrasch, S., Bullough, P. A., Ghosh, R. (1995) The 8.5 Å projection map of the light-harvesting complex I from *Rhodospirillum rubrum* reveals a ring composed of 16 subunits, *EMBO J. 14*, 631-638.

34. McLuskey, K., Prince, S. M., Cogdell, R.J., Isaacs, N.W. (2001) The crystallographic structure of the B800-820 LH3 light-harvesting complex from the purple bacteria *Rhodopseudomonas acidophila* strain 7050, *Biochemistry 40*, 8783-8789.

35. Ritz, T., Park, S., Schulten, K. (2001) Kinetics of excitation migration and trapping in the photosynthetic unit of purple bacteria, *J. Phys. Chem. B* 105, 8259-8267.

36. Deisenhofer, J., Epp, O., Miki, K., Huber, R., Michel, H. (1985) X-ray structure analysis at 3 Å resolution of a membrane protein complex: folding of the protein subunits in the photosynthetic reaction centre from *Rhodopseudomonas viridis, Nature 318*, 618-624.

37. McDermott, G., Prince, S. M., Freer, A. A., Hawthornthwaite-Lawless, A. M., Papiz, A. M., Cogdell, R. J., Isaacs, N.W. (1996) Crystal structure of an integral membrane light-harvesting complex from photosynthetic bacteria, *Nature 374*, 517-521.

38. Walz,T., Jamieson, S.J., Bowers, C.M., Bullough, P.A., Hunter, C.N. (1998) Projection structures of three photosynthetic complexes from *Rhodobacter sphaeroides:* LH2 at 6 Å , LH1 and RC-LH1 at 25 Å, *J. Mol. Biol. 282*, 833-845.

39. Hess, S., Chachisvilis, M., Timpmann, K., Jones, M.R., Fowler, G.J.S., Hunter, C., Sundström, V. (1995) Temporally and spectrally resolved subpicosecond energy transfer within the peripheral antenna complex (LH2) and from LH2 to the core antenna complex in photosynthetic purple bacteria, *Proc. Natl. Acad. Sci., U.S.A. 92,* 12333-12337.

40. Timpmann, K., Freiberg, A., Sundström, V. (1995) Energy trapping and detrapping in the photosynthetic bacterium *Rhodopseudomonas viridis*: transfer-to-trap limited dynamics, *Chem. Phys. 194*, 275-283.

41. Förster, T. (1948) Zwischenmolekulare Energiewanderung und Fluoreszenz, *Annal. der Physik* 6, 55-75.

42. Pullerits, T., Hess, S., Herek, J.L, Sundström, V. (1997) Temperature dependence of excitation transfer in LH2 of *Rhodobacter sphaeroides. J. Phys. Chem. B 101*, 10560-10567.

43. Scholes, G.D.; Fleming, G.R. (2000) On the mechanism of light-harvesting in photosynthetic purple bacteria: B800 to B850 energy transfer, *J. Phys. Chem. B 104*, 1854-1868.

44. Sumi, H. (1999) Theory on rates of excitation-energy transfer between molecular aggregates through distributed transition dipoles with application on the antenna system in bacterial photosynthesis, *J. Phys. Chem. B 103*, 252-260.

45. Linnanto, J., Korppi-Tommola, J.E.I. (2000) Excitation energy-transfer in the LH2 antenna of photosynthetic purple bacteria via excitonic B800 and B850 states, *J. Chin. Chem. Soc. 47*, 657-665.

46. Gradinaru, C. C., Kennis, J. T. M., Papagiannakis, E., van Stokkum, I. H. M., Cogdell, R. J., Fleming, G. R., Niederman, R. A., van Grondelle, R. (2001) A new pathway of excitation energy deactivation in carotenoids: singlet to triplet conversion on an ultrafast time scale in a photosynthetic antenna, *Proc. Natl. Acad. Sci. USA 98*, 2364-2369.

47. Macpherson, A.N., Arellano, J.B., Fraser, N.J., Cogdell, R.J., Gillbro, T. (2001) Efficient energy transfer from the carotenoid S_2 state in a photosynthetic light-harvesting complex, *Biophys J. 80*, 923-930.

48. Walla, P.J., Linden, P.A., Hsu, C.-P., Scholes, G.D., Fleming, G.R. (2000) Femtosecond dynamics of the forbidden carotenoid S1 state in light-harvesting complexes of purple bacteria observed after two-photon excitation, *Proc. Natl. Acad. Sci U.S.A. 97*, 10808-10813.

49. Chitnis, P. R. (2001) Photosystem I: Function and physiology, *Ann. Rev. Plant Physiol. Plant Mol. Biol. 52*, 593-626.

50. Scheller, H. V., Jensen, P. E., Haldrup, A., Lunde, C., Knoetzel, J. (2001) Role of subunits in eukaryotic photosystem I, *Biochim. Biophys. Acta 1507*, 41-60.

51. Fromme, P., Jordan, P., Krauss, N. (2001) Structure of photosystem I, *Biochim. Biophys. Acta 1507*, 5-31.

52. Boekema, E. J., Jensen, P. E., Schlodder, E., van Breemen, J. F. L., van Roon, H., Scheller, H. V., Dekker, J.P. (2001) Green plant photosystem I binds light-harvesting complex I on one side of the complex, *Biochemistry 40*, 1029-1036.

53. Croce, R., Zucchelli, G., Garlaschi, F.M., Jennings, R.C. (1998) A thermal broadening study of the antenna chlorophylls in PSI-200, LHCI, and PSI core, *Biochemistry 37*, 17355-17360.

54. Jensen, P. E., Gilpin, M., Knoetzel, J., Scheller, H. V. (2000) The PSI-K subunit of photosystem I is involved in the interaction between light-harvesting complex I and the photosystem I reaction center core, *J. Biol. Chem. 275*, 24701-24708.

55. Kruip, J., Boekema, E.J., Bald, D., Boonstra, A.F., Rögner, M. (1993) Isolation and structural characterization of monomeric and trimeric photosystem I complexes (P700 FA/FB and P700 FX) from the cyanobacterium *Synechcystis PCC 6803*, *J. Biol. Chem. 268*, 23353-23360.

56. Sun, J., Ke, A., Jin, P., Chitnis, V.P., Chitnis, P.R. (1998) Isolation and functional study of photosystem I subunits in the cyanobacterium Synechocystis sp. PCC 6803, *Methods Enzymol.* 297, 124-139.

57. Schmid, V.H.R., Cammarata, K.V., Bruns, B.U., Schmidt G.W. (1997) *In Vitro* reconstitution of the photosystem I light-harvesting complex LHCI-730: Heterodimerization is required for antenna pigment organization, *Proc. Natl. Acad. Sci U.S.A. 94*, 7667-7672.

58. Gobets, B., van Grondelle, R. (2001) Energy transfer and trapping in photosystem I, *Biochim. Biophys. Acta 1507*, 80-99.

59. Du, M., Xie, X., Jia, Y., Mets, L., Fleming, G.R. (1993) Direct observation of ultrafast energy transfer in PSI core antenna, *Chem. Phys. Lett. 201*, 535-542.

60. Kennis, J. T. M., Gobets, B., van Stokkum, I. H. M., Dekker, J.P., van Grondelle, R. Fleming, G.R. (2001) Light harvesting by chlorophylls and carotenoids in the photosystem I core complex of Synechococcus elongatus: a fluorescence upconversion study, *J. Phys Chem. B. 105*, 4485-4494.

61. Gobets, B., Kennis, J. T. M. , Ihalainen, J. A., Brazzoli, M., Croce, R., van Stokkum, I. H. M., Bassi, R., Dekker, J. P., van Amerongen, H., Fleming, G. R., van Grondelle, R. (2001) Excitation energy transfer in dimeric light-harvesting complex I: a combined streak-camera/ fluorescence upconversion study, *J. Phys. Chem. B. 105*, 10132-10139.

62. Gradinaru, C. C., Pascal, A.A., van Mourik, F., Robert, B., Horton, P., van Grondelle, R. van Amerongen, H. (1998) Ultrafast evolution of the excited states in the chlorophyll *a/b* complex CP29 from green plants studied by energy-selective pump-probe spectroscopy, *Biochemistry 37*, 1143-1149.

63. Melkozernov, A.N. (2001) Excitation energy transfer in photosystem I from oxygenic organisms, *Photosynth. Res. 70*, 129-153.

64. Gibasiewicz, K., Ramesh, V. M., Melkozernov, A. N., Lin, S., Woodbury, N. W., Blankenship, R. E., Webber, A. N. (2001) Excitation dynamics in the core antenna of PS I from *Chlamydomonas reinhardtii CC 2696* at room temperature, *J. Phys. Chem. B. 105*, 11498-11506.

65. Croce, R., Dorra, D., Holzwarth, A. R., Jennings, R. C. (2000) Fluorescence decay and spectral evolution in intact photosystem I of higher plants, *Biochemistry 39*, 6341-6348.

66. Kumazaki, S., Ikegami, I., Furusawa, H., Yasuda, S., Yoshihara,K. (2001) Observation of the excited state of the primary electron donor chlorophyll (P700) and the ultrafast charge separation in the spinach photosystem I reaction center, *J. Phys. Chem. B 105*, 1093-1099.

67. Melkozernov, A. N., Schmid, V. H. R., Schmidt, G. W., Blankenship, R. E. (1998) Energy redistribution in heterodimeric light-harvesting complex LHCI-730 of photosystem I, *J. Phys. Chem. B. 102*, 8183-8189.

68. Werst, M.M., Jia Y., Mets, L., Fleming, G.R. (1992) Energy transfer and trapping in the pPSI core antenna , a temperature study, *Biophys. J. 61*, 868-878.

69. Karapetyan, N.V., Holzwarth, A.R., Rögner, M. (1999) The photosystem I trimer of cyanobacteria: molecular organization, exciton dynamics and physiological significance, *FEBS Lett. 460*, 395-400.

70. Rivadossi, A., Zucchelli, G., Garlaschi, F.M., Jennings, R.C. (1999) The importance of PS I chlorophyll red forms in light-harvesting by leaves, *Photosynth. Res.* 60, 209-215.

71. Trissl, H.-W., Wilhelm, C. (1993) Why do thylakoid membranes from higher plants form grana stacks? *Trends in Biochem. Sci. 18*, 415-419.

72. Giuffra, E., Cugini, D., Croce, R., Bassi, R. (1996) Reconstitution and pigment-binding properties of recombinant CP29, *Eur. J. Biochem. 238*, 112-120.

73. Paulsen, H., Rümler, U., Rüdiger, W. (1990) Reconstitution of pigment-containing complexes from light-harvesting chlorophyll a/b-binding proetin overexpressed in *Escheria coli*, *Planta 181*, 204-211.

74. Fowler, G.J.S., Visschers, R.W., Grief, G.G., van Grondelle, R., Hunter, C.N. (1992) Genetically modified photosynthetic antenna complexes with blueshifted absorbance bands. *Nature 355*, 848-850.

75. Fraser, N.J., Dominy, P.J., Ücker, B., Simonin, I., Scheer, H., Cogdell, R.J. (1999) Selective release, removal, and reconstitution of BChla molecules into B800 sites of LH2 complexes from *Rhodopseudomonas acidophila* 10050, *Biochemistry 38*, 9684-9692.

76. Zouni, A., Witt, H.-T., Kern, J., Fromme, P., Krauss, N., Saenger, W., Orth, P. (2001) Crystal structure of photosystem II from *Synechococcus elongatus* at 3.8 Å resolution, *Nature 409*, 739-743.

77. Mukamel, S. (1999) *Principles of nonlinear optical spectroscopy.* Oxford University Press, New York.

78. Agranovich, V.M., Hochstrasser, R.M. (eds) (1983) Chapter 8 (Theory of light absorption and emission by organic impurity centers, I.S. Osad'ko), Chapter 10 (Site selection spectroscopy of complex molecules in solutions and its applications, R.I. Personov) in *Spectroscopy and Excitation Dynamics of Condensed Molecular Systems*, North-Holland Publishing Company, Amsterdam.

79. Amesz, J., Hoff, A.J., (eds) (1996) Chapters 1 (Classical optical spectroscopy, J. Amesz), Chapter 2 (Linear and circular dichroism, G. Garab), Chapter 3 (Fluorescence, K. Sauer & M. Debreczeny), Chapter 4 (Ultrafast spectroscopy of photosynthetic systems, R. Jimnez & G. Fleming), Chapter 5 (Data analysis of time-resolved measurements, A. Holzwarth), in *Biophysical Techniques in Photosynthesis*, Kluwer Academic Publisher, Dordrecht.

80. van Gurp, M., van der Heide, U., Verhagen, J., Piters, T., van Ginkel, G., Levine, Y.K. (1989) Spectroscopic and orientational properties of chlorophyll *a* and chlorophyll *b* in lipid membranes, *Photochem. Photobiol. 49*, 663-672.

81. van Zandvoort, M.A.M.J., Wrobel, D., Lettinga, P., van Ginkel, G., Levine, Y.K. (1995) The orientation of the transition dipole moments of chlorophyll *a* and pheophytin *a* in their molecular frame, *Photochem. Photobiol. 62*, 299-308.

82. van Amerongen, H., Kwa, S.L.S., van Bolhuis, B.M., van Grondelle, R. (1994) Polarized fluorescence and absorption of macroscopically aligned light harvesting complex II. *Biophys. J.* 67, 837-847.

83. van der Lee, J. , Bald, D., Kwa, S.L.S., van Grondelle R., Rögner M.Dekker J.P. (1993) Steady-state polarized light spectroscopy of isolated photosystem I particles. *Photosynth. Res. 35*, 311-321.

84. Simonetto, R., Crimi, M., Sandonà, D., Croce, R., Cinque, C., Breton, J., Bassi, R. (1999) Orientation of chlorophyll transition moments in the higher-plant light-harvesting complex CP29, *Biochemistry* 38, 12974-12983.

85. Lakowicz, J.R. (1983) Principles of fluorescence spectroscopy. Plenum, New York.

86. Rebane, K.K. (1988) Zero-phonon lines in the spectroscopy and photochemistry of impurity-doped solid matter, Chpater 1 in *Zero-phonon lines and spectral hole-burning in spectroscopy and photochemistry*, Sild, O., Haller, K. (Eds). Springer Verlag Berlin Heidelberg.

87. Jankowiak, R., Hayes, J.M., Small, G.J. (1993) Spectral hole-burning spectroscopy in amorphous molecular solids and proteins, *Chem. Rev. 93*, 1471-1502.

88. Reinot, T., Zazubovich, V., Hayes, J.M., Small, G. (2001) New insights on persistent non-photochemical hole burning and its applications to photosynthetic complexes. *J. Phys. Chem. B 105*, 5083-5098.

89. Hayes, J.M., Gillie, J.K., Tang, D., Small, G.J. (1988) Theory for spectral hole-burning of the primary electron donor state of photosynthetic reaction centers, *Biochim. Biophys. Acta 932*, 287-305.

90. Pieper, J., Voigt, J., Renger, G., Small, G.J. (1999) Analysis of phonon structure in line-narrowed optical spectra, *Chem. Phys. Lett. 310*, 296-302.

91. Sutherland, R.L. (1996) *Handbook of Nonlinear Optics.* Marcel Dekker Inc, New York.

92. Rulliere, C. (1998) *Femtosecond Laser Pulses, Principles and Experiments.* Springer-Verlag, Berlin Heidelberg.

93. O'Connor, D.V., Phillips, D. (1984) *Time-Correlated Single Photon Counting.* Academic Press, London.

94. Bassi, R., Simpson, D. (1987) Chlorophyll-protein complexes of barley photosystem I, *Eur. J. Biochem. 163*, 221-230.

95. Croce, R., Bassi, R. (1998) The light-harvesting complex of photosystem I: pigment composition and stoichiometry In *Photosynthesis: Mechanisms and Effects,* Garab, G. (ed), *Vol. I*, p. 421-424, Kluwer Academic Publishers, the Netherlands.

96. Ganeteg, U., Strand, Å., Gustafsson, P., Jansson S. (2001) The Properties of the chlorophyll a/*b*-binding proteins Lhca2 and Lhca3 studied *in vivo* using antisense inhibition, *Plant Physiology* 127, 150-158.

97. Lunde, C., Jensen, P. E., Haldrup, A., Knoetzel, J., Scheller, H. V. (2000) The PSI-H subunit of photosystem I is essential for state transitions in plant photosynthesis, *Nature 408*, 613-615.

98. Jensen, P. E., Rosgaard, L., Knoetzel, J., Scheller, H.V. (2002) Photosystem I activity is increased in the absence of the PSI-G subunit, *J. Biol. Chem.* 277, 2798-2803.

Paper I

https://doi.org/10.1021/jp010921b

Paper II

https://doi.org/10.1021/bi0007369

Paper III

A manuscript of "Phonon couplings of red chlorophyll states of green plant PSI complex - a site-selective spectroscopy study" Ihalainen, J.A., Rätsep, M., Jensen, P.E., Scheller, H.V., Croce, R., Bassi, R., Freiberg, A., Korppi-Tommola, J.E.I. To be submitted.

https://doi.org/10.1021/jp034778t

Paper IV

https://doi.org/10.1016/S0006-3495(02)73979-9